Ministry of Education and Science of Ukraine
Bohdan Khmelnytsky National University of Cherkasy
Institute of Organic Chemistry of NAS of Ukraine
Lviv Polytechnic National University, Ukraine
V. N. Karazin Kharkiv National University, Ukraine
L. V. Pisarzhevsky Institute of Physical Chemistry
of NAS of Ukraine
KTH Royal Institute of Technology, Stockholm, Sweden
L. N. Gumilyov Eurasian National University,
Republic of Kazakhstan
University of Copenhagen, Denmark
Norwegian National University of Science and Technology,
Trondheim, Norway
Crop Care Institute, UKRAVIT Corporation

BOOK OF ABSTRACTS

International Scientific Conference

MOLECULAR ENGINEERING AND COMPUTATIONAL MODELLING FOR NANO- AND BIOTECHNOLOGY: FROM NANOELECTRONICS TO BIOPOLYMERS

dedicated to the 75th anniversary of
Professor Boris Minaev

September 25–26, 2018, Cherkasy, Ukraine

Cherkasy – 2018

UDK 620.3 : 544.18 (062.552)
I69

International Scientific Conference: «Molecular Engineering and Computational Modelling for Nano- and Biotechnology: From Nanoelectronics to Biopolymers», September 25–26, 2018, Cherkasy, Ukraine. Book of Abstracts. Cherkasy : Chabanenko Yu. A., 2018. – 152 p.
ISBN 978-966-920-350-2

The book of abstracts contains results of scientific works devoted to the fundamental and applied problems of materials science, organic electronics and biotechnology, as well as the design of multilayer devices and the problems of the theory of charge transfer and excitation, luminescence on the interface, the manufacture of multilayer devices.

UDK 620.3 : 544.18 (062.552)

Recommended for publication by the Scientific Council of the Bohdan Khmelnytsky Cherkasy National University
(protocol No. 1 dated 30 August, 2018)

ISBN 978-966-920-350-2

УДК 620.3 : 544.18 (062.552)
І69

Міжнародна наукова конференція: «Молекулярна інженерія та комп'ютерне моделювання для нано- і біотехнологій: від наноелектроніки до біополімерів», 25–26 вересня, 2018, Черкаси, Україна. Збірник тез. Черкаси : Вид. Чабаненко Ю. А., 2018. – 152 с.
ISBN 978-966-920-350-2

У збірнику наведено матеріали наукових робіт, присвячених фундаментальним і прикладним проблемам матеріалознавства, органічної електроніки і біотехнології, а також питанням теорії перенесення заряду і збудження, люмінесценції на інтерфейсі, виготовленню багатошарових пристроїв.

УДК 620.3 : 544.18 (062.552)

Рекомендовано до друку Вченою радою Черкаського національного університету імені Богдана Хмельницького
(протокол № 1 від 30 серпня 2018 р.)

ISBN 978-966-920-350-2

PROGRAM COMMITTEE

Cherevko O. V. – Committee Chairman, Rector of the Bohdan Khmelnytsky National University, Cherkasy (ChNU)
Kornovenko S. V. – Vice-Rector for Scientific, Innovation and International Activities, ChNU
Moysienko V. M. – First Vice-Rector, ChNU
Gavrilyuk G. M. – Vice-Rector on Educational Work and Prestige-Development Activity, ChNU
Udovenko Yu. G. – Vice-Rector for Administrative and Economic Activity, ChNU
Ishchenko A. A. – Corresponding Member of NAS of Ukraine, Head of the Department of Colour and Structure of Organic Compounds, Institute of Organic Chemistry of NAS of Ukraine
Mchedlov-Petrossyan N. O. – Corresponding Member of NAS of Ukraine, Head of the Physical Chemistry Department, V. N. Karazin Kharkiv National University
Kuchmy S. Ya.– Corresponding Member of NAS of Ukraine, Head of the Photochemistry Department, L. V. Pisarzhevsky Institute of Physical Chemistry of NAS of Ukraine
Pittelkow M. – Head of the Laboratory of Organic and Supramolecular Chemistry, University of Copenhagen, Denmark
Ågren H. – Professor of the Department of Theoretical Chemistry and Biology, KTH Royal Institute of Technology, Stockholm, Sweden
Stakhira P. Y. – Professor of the Department of Electronic Devices, Lviv Polytechnic National University, Ukraine
Irgibayeva I. S. – Professor of the Chemistry Department, L. N. Gumilyov Eurasian National University, Astana
Lindgren M. – Professor of the Department of Physics, Norwegian National University of Science and Technology, Trondheim

ORGANIZING COMMITTEE

Gavrilyuk M. N. – Director of the Natural Sciences Institute, ChNU

Minaeva V. O. – Docent of the Chemistry and Nanomaterial Science Department, ChNU

Boiko V. I. – Docent of the Chemistry and Nanomaterial Science Department, ChNU

Karaush-Karmazin N. M. – PhD. scientist of the Chemistry and Nanomaterial Science Department, ChNU

Lut O. A. – Docent of the Chemistry and Nanomaterial Science Department, ChNU

Baryshnikov G. V. – PhD., Department of Theoretical Chemistry and Biology, KTH Royal Institute of Technology, Stockholm, Sweden

Gusak A. M. – Professor of the Physics Department, ChNU

Norman P. – Head of the Department of Theoretical Chemistry and Biology, KTH Royal Institute of Technology, Stockholm, Sweden

Shafranyosh I. I. – Head of the Quantum Electronics Department, Uzhgorod National University, Ukraine

Zaichenko A. S. – Professor of the Organic Chemistry Department, Lviv Polytechnic National University, Ukraine

Ilchenko V. V. – Head of the Crop Care Institute, UKRAVIT Corporation

Ostapenko N. I. – Professor of the Photoactivity Division, Institute of Physics, NAS of Ukraine

Sakhno T. V. – Professor of the Trade and Economics University, Poltava, Ukraine

CONTENTS

BORIS F. MINAEV – A PRIME SCHOLAR, SCIENTIFIC SPECIALIST AND CREATOR

Hans Ågren

Department of Theoretical Chemistry and Biology, Royal Institute of Technology, SE-10609 Stockholm, Sweden

e-mail: hagren@kth.se

I will highlight a selection from the great pool Boris F. Minaevs scientific work, giving some personal reflections on their importance in general and for Swedish Theoretical Chemistry.

Fig. 1. The detailed origin of the green Aurora was explained by Boris Minaev.

References

1. B. F. Minaev et al, *Chem. Phys. Letters*, 1995, **231**, 387.

NANOELECTRONICS AND QUANTUM ENZYMOLOGY IN CHERKASY

Boris Minaev

Department of Chemistry and Nanomaterials Science, Bohdan Khmelnytsky National University, 18031, Cherkasy, Ukraine, e-mail: bfmin43@ukr.net

Scientific projects of our department embrace wide interests in modern frontiers of natural sciences. All projects are based on molecular engineering at nano-level and computational modeling of artificial atomic ensembles, nano-clusters, molecular complexes, exciplexes, oligomers and protein aggregates. In this talk I present two examples connected with OLED fabrication and modeling of recently discovered class of enzymes – mono- and di-oxygenases which activate dioxygen being lack of any cofactor or transition metal. The O_2 molecule (dioxygen) possesses the triplet ground state and can not react with diamagnetic organic stuff which has all spin paired. One possible way to overcome spin forbidden character of such reactions includes initiation of radical chain processes since reaction of dioxygen with radical is spin-allowed in the doublet common spin state. Such radical reactions of the combustion type are not appropriate for the living cell. Meanwhile, mono- and di-oxygenases incorporate one or two atoms of O_2 molecule into organic substrates. How they overcome the spin prohibition (especially in the absence of

any cofactor or metal ions) – is a great puzzle in modern enzymology. Now we solved this puzzle by quantum modeling of HOD enzyme [1-3]. Thus, the bacterial 2,4-dioxygenase HOD (1-*H*-3-hydroxy-4-oxoquinaldine 2,4-dioxygenase) has no cofactor, but catalyzes the triplet O_2 reaction with the N-heterocyclic substrate (2-methyl-3-hydroxy-4(1*H*)-quinolone, MHQ), denoted here as SH, and produces CO + N-acetyl-anthranilate

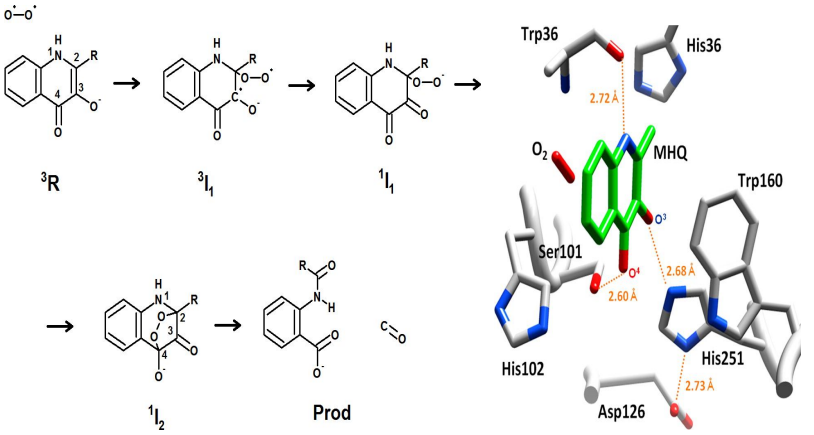

(a) (b)

Fig. 1. The mechanism of HOD catalyzed reaction with 2-n-alkyl-3-hydroxy-4(1*H*)-quinolones proposed and discussed in Refs. [1, 2] (a); HOD active cite model (NAA) products, Fig 1.a [1, 2] (b).

According to Ref. 1 a direct O_2 attack on substrate S$^-$ anion leads to a covalently-bound $^3I_1$ triplet intermediate through a large barrier of 17.4 kcal/mol (Fig 1). The spin inversion between $^3I_1$ and $^1I_1$ would occur at the minimum

energy crossing point (MECP) [1]. The authors [1] have not achieved the MECP optimization in their DFT study and have not discussed the driving force for T-S transition. We have optimized this MESP by CASSCF method and found that spin-orbit coupling (SOC) matrix element between $^3I_1$ and $^1I_1$ states at this crossing point is close to zero (2.7 cm^{-1}). Thus, we support the thermochemistry DFT calculations of Pedro Silva [2] who rejected the direct O_2 attack and the $^3I_1$ intermediate formation on the ground of preference for the electron-transfer mechanism $^3R(S^- + {}^3O_2) \rightarrow {}^3(S^{\bullet} \ldots O_2^{-\bullet})$. The formed triplet radical pair between substrate radical and superoxide ion inside proteins pocket of HOD (Fig. 1b) is more favorable than peroxy-biradical $^3I_1$ (Fig. 1a) by 8 kcal/mol. Moreover, we have shown [4, 5] that the SOC integral between triplet and singlet states of the $^{3,1}(S^{\bullet} \ldots O_2^{-\bullet})$ radical pair achieves the maximum possible value of 80 cm^{-1}, which provides an effective spin flip and transfer into the $^1I_1$ intermediate. The rest of reaction follows the traditional zero-spin-chemistry pathway, shown by Fig. 1.a, which was correctly described by DFT simulations [1, 2].

NANOELECTRONICS: Hetero[8]circulenes Expedient Synthesis for OLEDs

In the second part of my talk I shall present the new materials design for OLED fabrication. They are described in a book (Fig. 2b) and we are very proud of it [6].

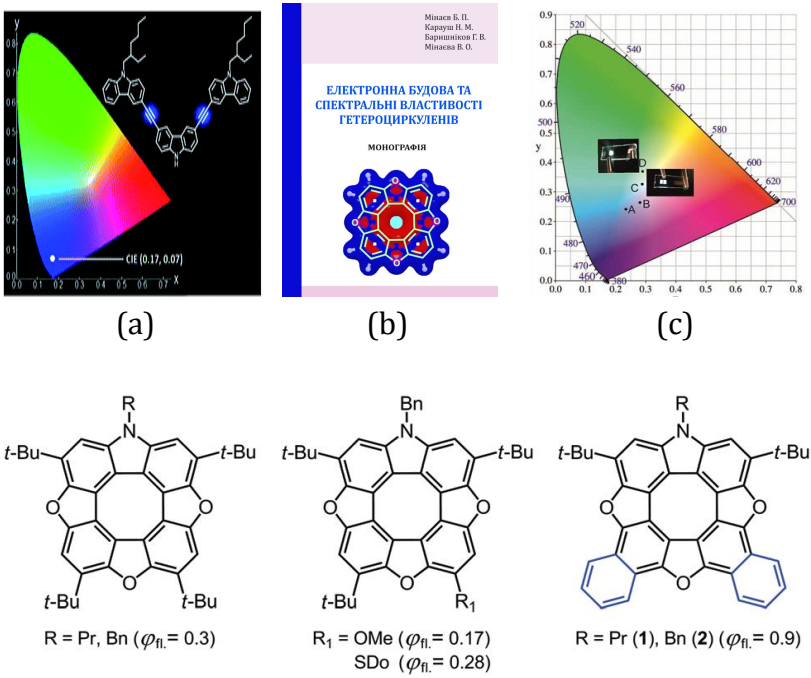

(a) (b) (c)

(d) (e) (f)

Fig. 2. Chromaticity diagrams (a, c) for various OLED; (b) the first comprehensive description of hetero[8]circulenes and their representatives used in OLED design (d–f).

Azatrioxa[8]circulenes (Fig. 2 d–f) are the most efficient fluorophors: eliminations of inversion symmetry strongly reduce the electric dipole selection rule and provides fluorescence with high quantum yield [7, 8]. The star-shaped m-MTDATA molecule forms exciplex with our circulenes (Fig. 2 f) at the interface; this affords to fabricate a number of OLED devices (Fig. 3) with good brightness (23700 Cd/m^2 at 15 V, current efficiency 4.2 Cd/A) and

white color: points C (0.27, 0.33) and D (0.28, 0.36) of the CIE1931 standard in Fig. 2 c. Quantum EQE is about 3% (C) can be improved.

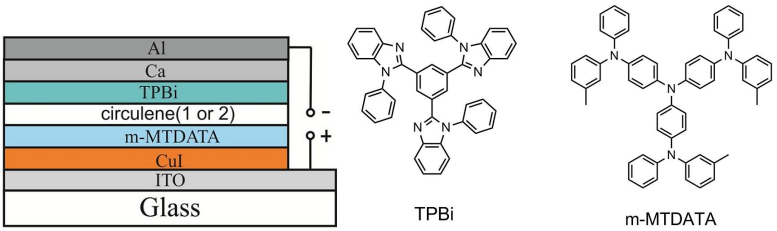

Fig. 3. The structure of OLEDs with benzimidazole derivative (TPBi) as an elecron-transport layer and tris[phenyl(m-tolyl)amino]triphenylamine (m-MTDARA) as a hole-transport layer [7].

Thus, the presented examples illustrate some typical features of our projects. One can image that all studies of our department involve huge variety of spin-orbit coupling effects in OLED technology, spin catalysis, dye-sentisized solar cells, magnetic and optical properties of organic and inorganic materials [8], and, in particular, – in quantum enzymology [4, 5]. Photo- and bio-activation of dioxygen with account of SOC effects is in the center of our biomedical and agricultural efforts (reactive oxygen species as signaling redox systems in plants) [9]. The SOC theory developed for glucose oxidase [4, 5] is generalized here to all flavin cofactor-containing enzymes which activate dioxygen. It is stressed that SOC is determined by the open shell of superoxide and does not depend on cofactor. That is

why the old theory [4, 5] can be applied for cofactor-independent oxygenases.

References

1. A. Hernandez-Ortega, M. G. Quesne, S. Bui, D. J. Heyes, R. A. Steiner, N. S. Scrutton, S. P. de Visser, *J. Am. Chem. Soc.*, 2015, **137**, 7474.
2. P. J. Silva, *Peer J.*, 2016, **4** (12), e2805.
3. S. Bui, R. A. Steiner, *Current Opinion Struct. Biol.*, 2016, **41**, 109.
4. B. F. Minaev, *RIKEN Rev*., 2002, **44**, 147.
5. B. F. Minaev, *Russ. Chem. Rev.*, 2007, **76**, 988.
6. Electronic structure and spectral properties of heterocirculenes: monograph // B. F. Minaev, N. N. Karaush, G. V. Baryshnikov, V. A. Minaeva. – Cherkasy, 2017, 264 p. (*in Ukrainian*).
7. K. B. Ivaniuk, G. V. Baryshnikov, P. Y. Stakhira, S. K. Pedersen, M. Pittelkow, A. Lazauskas, D. Volyniuk, J. V. Grazulevicius, B. F. Minaev, H. Ågren, *J. Mat. Chem. C*, 2017, **5**, 4123.
8. G.V. Baryshnikov, B.F. Minaev, H. Ågren, *Chem. Rev.*, 2017, **117**, 6500.
9. M. Bregnhøj, M. Westberg, B. F. Minaev, P. R. Ogilby, *Acc. Chem. Res.*, 2017, **50**, 1920.

CALCULATION OF VIBRATIONAL FREQUENCIES AND INTENSITIES OF IR ABSORPTION BANDS OF MESOGENIC BIPHENYLS

L. K. Abulyaissova, R. V. Barannikov and M. T. Alimbayeva

Faculty of Chemistry, Buketov State University, 100028, Karaganda, Kazakhstan,
e-mail: abu.lyazzat@gmail.com

Technologically the most important mesophase is the nematic liquid crystal phase. Nematic liquid crystals are used in optical electronics, gas-liquid chromatography, thermography and multicomponent systems study.

When studying mesogenic compounds, a variety of experimental and theoretical methods are used. The development of effective quantum mechanical computational methods has made it possible to calculate many molecular properties.

In our researches geometrical and electronic structure, infrared spectrum, thermodynamic properties of the compounds are investigated by means of the force field, HF and DFT quantum mechanical methods with the split-valence basis sets including polarization and diffuse functions. Various possible conformers, rotation potentials, and transition states for the mesogenic compounds with different polar and non-polar substituents are predicted computationally [1–4].

The application of quantum chemical methods provides the prediction of the frequencies and types of normal vibrations along with the intensities of IR bands for the stretching, moderate- and low-frequency regions of the spectrum.

The forms of stretching vibrations, their frequencies and intensities of the IR absorption bands of liquid crystalline biphenyls were calculated theoretically by the density functional method with the Becke 3 Lee Yang Parr correlation functional (DFT/B3LYP) [5, 6] with the 6-31G(d) basis (Fig. 1, 2).

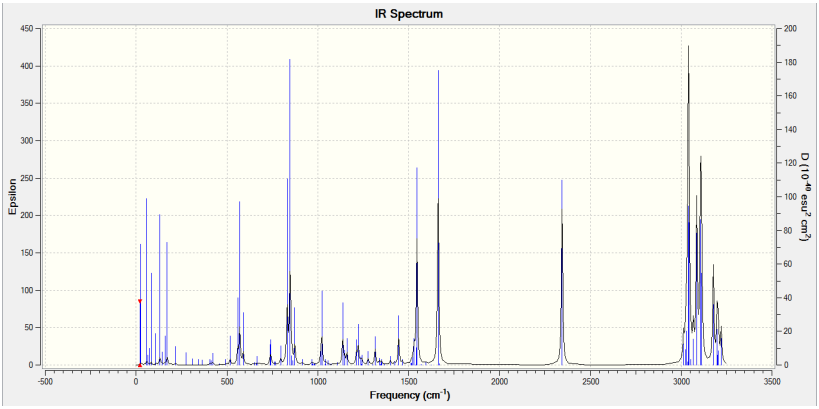

Fig. 1. The theoretical quantum chemical vibrational spectrum (in the *absorption coefficient –frequency* coordinates) of 4-*n*-pentyl-4'-cyanobiphenyl molecule.

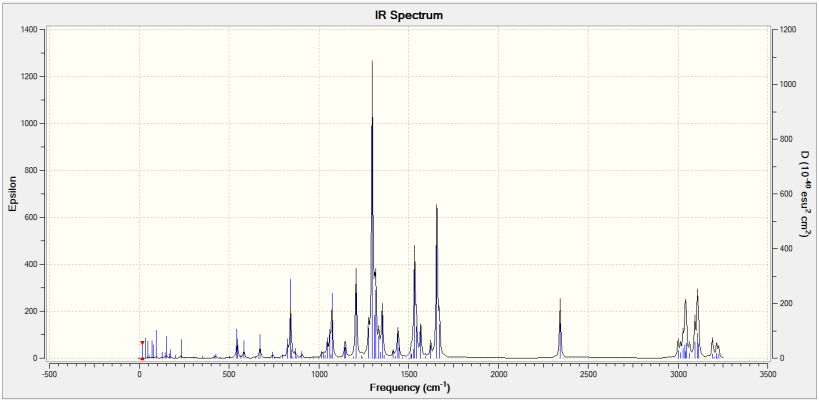

Fig. 2. The theoretical vibrational spectrum of 4-pentoxy-4'-cyanobiphenyl molecule.

References

1. L. K. Abulyaissova *et al., 15th Intern. Congress Quant. Chem.: Book Abstr.*, Beijing, 2015, 42.
2. L. Abulyaissova and M. Alimbayeva, *26th International Liquid Crystal Conference: Book Abstr.*, Kent, 2016, 371.
3. L. K. Abulyaissova, S. O. Kenzhetaeva, M. S. Kasymova, *Russian Journal of General Chemistry*, 2017, **87**, 1125.
4. L. K. Abulyaissova, *27th International Liquid Crystal Conference: Book Abstr.*, Kyoto, 2018.
5. A. D. Becke, *J. Chem. Phys*., 1993, **98**, 5648.
6. M. J. Frisch, G. W. Trucks, H. B. Schlegel *et al*. *GAUSSIAN 09*, Revision A.02. – Wallingford CT, 2009.

DFT CALCULATION OF 3-PHENYL-5-NITROMETHYL-4,5-DIHYDROISOXAZOLE

Dmytro Babyuk[1], Radomir Jasinski[2] and Yaryna Motovylina[1]

[1]Institute of Biology, Chemistry and Bioresources, Yuriy Fedkovych Chernivtsi National University, 58012, Chernivtsi, Ukraine,
e-mail: d.babyuk@chnu.edu.ua
[2]Institute of Organic Chemistry and Technology, Cracow University of Technology, 31-155, Cracow, Poland

4,5-Dihydroisoxazoles are heterocycles with many important practical applications. There are many efficient methods for preparation of nitrosubstituted 4,5-dihydroisoxazoles; the most universal one is [3+2] cycloaddition between nitrile N-oxides and conjugated nitroalkenes. At the same time, nitromethyl-substituted 4,5-dihydroisoxazole are very poorly studied. Herein, we present the quantum chemical results of 3-phenyl-5-nitromethyl-4,5-dihydroisoxazole (**PNMDI**) computation [1].

The quantum-chemical calculations were performed using B3LYP functional with 6-31G(d) basis set implemented in the GAUSSIAN 09 package. The optimized structure of **PNMDI** along with natural bond analysis is shown in Fig. 1.

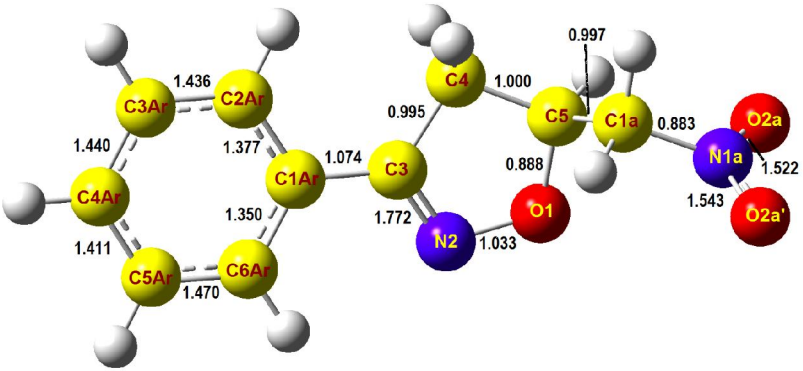

Fig. 1. Structure of **PNMDI** with computed bond orders.

Two –N=O bonds within the nitro group are not identical due to steric factors. The order of the C3=N2 bond in the isoxazole ring is only 1.772. This is caused by partial conjugation with the aromatic phenyl ring. Also the C3-C1Ar bond is denser than an ordinary single bond. At the same time, the aromatic bonds between C1Ar-C2Ar and C1Ar-C6Ar are weaker due to the conjugation. It agrees well with crystallographic results [1].

To model the UV-VIS spectrum, TDDFT/6-31G(d) calculation was carried out for 10 excited singlet states using PCM with methanol as a solvent. The maximum of the widest band in the experimental spectrum (Fig. 2) is located at 259 nm.

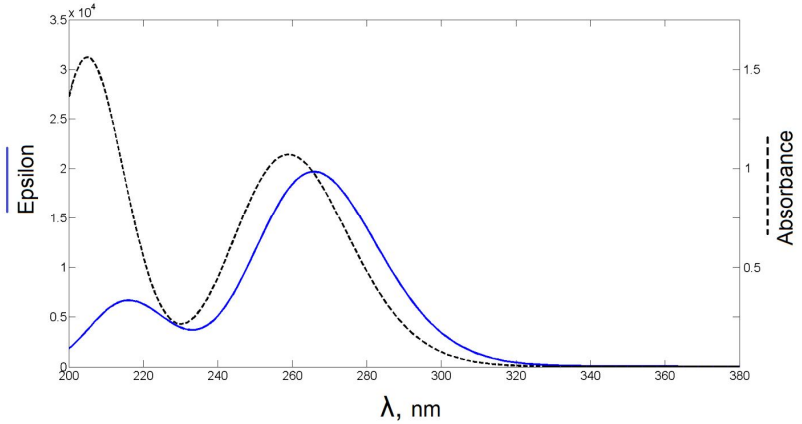

Fig. 2. Modeled, based on TDDFT calculation (solid), and experimental (dotted) UV spectrum of **PNMDI** taken in methanol.

The HOMO→LUMO transition is very weak with an oscillator strength value of 0.0012. It is barely seen in Fig. 2 at 350.23 nm. The experimental spectrum reveals the peak at 358 nm with an absorbance value of $3.4761 \cdot 10^{-4}$ AU. The strongest transition is found between HOMO and LUMO+1 with oscillator strength $f = 0.4772$. The corresponding wavelength is 265.97 nm. The left computed peak in Fig.2 located at 215.61 nm is due to the excited state consisting of 6 transitions. The largest contributions come from HOMO→LUMO+2 and HOMO-1→LUMO+1. In the experimental spectrum, this peak is located at 205 nm and is higher than the calculated one. However, within this level of computation, the results are quite satisfactory.

The IR-spectrum of **PNMDI** within the same theory level was computed as well. It is similar to the experimental

data. Besides NO_2 vibrations, there are also the most prominent N-O peaks within the isoxazole ring at 952.75 cm^{-1}, CH_2-bridge at 1397.10 cm^{-1}, and CH-stretch in the phenyl ring at 3203.53 cm^{-1}.

The results obtained from quantum chemical computations provide a valuable background for understanding the regiochemistry of formation of **PNMDI** in the [3 + 2] cycloaddition between benzonitrile N-oxide and 3-nitroprop-1-ene. They are also useful for better understanding of other [3+2] cycloaddition processes involving nitroallylic systems.

References

1. B. Mirosław, D. Babyuk, A. Łapczuk-Krygier, *et al. Monatsh Chem.,* 2018, https://doi.org/10.1007/s00706-018-2227-6.

THE RECENT PROGRESS IN COMPUTATIONS OF AROMATICITY AND PHOTOPHYSICAL PROPERTIES OF HETERO[8]CIRCULENES

Glib Baryshnikov

Department of Theoretical Chemistry and Biology,
KTH Royal Institute of Technology,
SE-10609 Stockholm
e-mail: glibar@kth.se

Owing to their potential use in organic light-emitting diodes [1] and field-effect transistors we report here the recent progress in computations of hetero[8]circulenes in order to explain the impact of outer substituents and benzoannelation on photophysical constants and aromaticity of these compounds in terms of spin-orbit coupling perturbation and magnetically-induced ring currents [2]. It is argued that the S_1–T_n inter-system crossing processes constitute the main deactivation pathways for the fluorescence quenching, something that is supported by a good agreement obtained with experimental data on fluorescence quantum yields. The concept of the gauge-including magnetically induced currents has been applied in order to estimate the role of substituents and benzoannelated fragments on the aromaticity and particularly on the overall balance between the diatropic “aromatic” and paratropic “antiaromatic” current strengths. While a variation of the substituents in the outer perimeter of the studied circulenes does not

provide a clear effect on their aromaticity, it is demonstrated that an additional benzoannelation (π-extension) of the azatrioxa[8]circulene macrocycle induces a significant aromaticity enhancement.

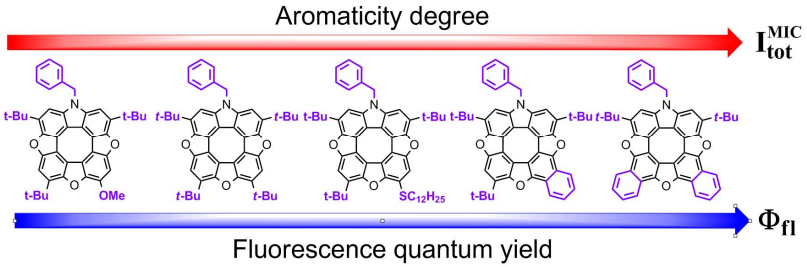

Fig. 1. Aromaticity *vs.* fluorescence quantum yield balance for the series of hetero[8]circulenes.

We have established the synergetic effect of benzoannelation and NH/O-substitution for enhancing the absorption intensity in a series of novel designed benzoannelated aza- and oxa[8]circulenes [3]. Semi-empirical estimations of the fluorescence rate constants allowed us to determine the most promising fluorophores among all the possible benzoannelated aza-, oxa- and mixed azaoza[8]circulenes. Among them, *para*-dibenzoannelated [8]circulenes demonstrated the most intense light absorption and emission due to the prevailing role of the linear acene chromophore. Calculated values of fluorescence quantum yield are in complete agreement with experimental data for a number of already synthesized circulenes. Thus, we believe that the most promising circulenes designed in this study can demonstrate an

intensive fluorescence in the case of their successful synthesis, which in turn could be extremely useful for the fabrication of future blue OLEDs [1, 3].

We also have explored the substituent-sensitive balance between fluorescence and non-radiative decay pathways as a tool for optical tuning of hetero[8]circulenes. Particulary, a series of *N*-butylated tetrabenzo-tetraaza[8]circulenes is studied computationally in order to explain the gradual decrease of fluorescence intensity with the increase of the substituent number [4].

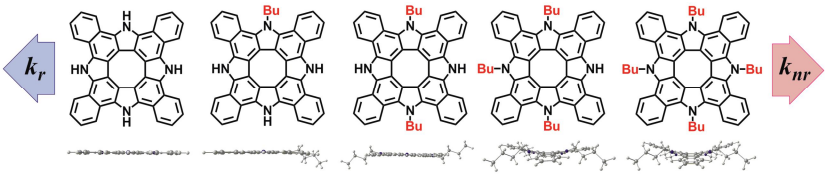

Fig. 2. Radiative *vs.* nonradiative rates balance depending on the number of outer Bu-substituents.

The inter-system crossing probability is found to increase upon the gradual substitution of the circulene macrocycle as a result of the decrease of the S_1–T_1 energy gap due to the deformation of the tetrabenzo-tetraaza[8]circulenes and therefore the distortion of the π-conjugation within the macrocycles. In contrast, the S_1–T_1 spin-orbit coupling matrix elements are quite insensitive to the number of outer substituents. As a result, the fluorescence-responsible ππ* transition becomes less intense and the fluorescence rate constant decreases.

References

1. K. B. Ivaniuk, G. V. Baryshnikov, P. Y. Stakhira, S. K. Pedersen, M. Pittelkow, A. Lazauskas, D. Volyniuk, J V. Grazulevicius, B. F. Minaev, H. Ågren, *J. Mater. Chem. C*, 2017, **5**, 4123.
2. G. V. Baryshnikov, R. R. Valiev, B. F. Minaev, H. Ågren, *New J. Chem.*, 2017, **41**, 7621.
3. G. V. Baryshnikov, R. R. Valiev, N. N. Karaush, V. A. Minaeva, A. N. Sinelnikov, S. K. Pedersen, M. Pittelkow, B. F. Minaev, H. Ågren, *Phys. Chem. Chem. Phys.*, 2016, **18**, 28040.
4. G. V. Baryshnikov, R. R. Valiev, B. F. Minaev, H. Ågren, *New J. Chem.*, 2017, **41**, 2717.

L_1-REGULARIZATION IN DIFFERENT APPLICATIONS OF CHEMICAL MODELING

Mykhailo I. Berdnyk, Vladimir V. Ivanov and Anton B. Zakharov

Materials Chemistry Department,
V. N. Karazin Kharkiv National University, 61022, Kharkiv, Ukraine,
e-mail: berdnikm@i.ua

Modern methods of material science need corresponding theoretical approaches for investigation and prediction of different molecular properties. Quantum chemistry and chemometric (*Quantity Structure-Activity Relationships*, QSAR) approaches are such methods. However, the general problem of real systems modeling is still not solved. Commonly it is connected with the complexity of real systems for which it is impossible to perform fairly precise calculations due to lack of computation recourses. Therefore, the current stage of new quantum chemical and chemometric methods development for purposes of practical material science requires approximations. One of the promising approaches for numerical simplification of corresponding equations is connected with the so-called "regularization" trick.

The general L_1-regularized equation has the following form:

$$\min_{z}\left(W(z)+\lambda\left\|z\right\|_1\right). \qquad (1)$$

Where $W(z)$ – is an initial function which should be minimized in order to obtain a solution of a corresponding problem, $\|z\|_1 = \sum_i |z_i| = \mathrm{sign}(z)^+ z$ is the L_1-norm of vector z and λ is the weight of penalty function. Inclusion of the L_1-norm makes it possible to reduce the size of z vector. It leads to the less computation-demanding approximation that is still capable to predict various chemical properties of molecules with proper accuracy.

The first application of L_1-regularization is connected with specific implementation of multilinear regression. In the present work we investigated capability of the L_1-regularized regression in comparison to different regression approaches in physical-chemistry parameters description. Among the **QSAR** regression models under study are *ordinary least squares* (**OLS**), *least absolute deviation* (**LAD**), *principle component regression* (**PCR**), *partial least squares* (**PLS**), *least absolute selection and shrinkage operator* (**LASSO**), *least angle regression stagewise*, (**LARS**), and *orthogonal distance regression* (**ODR**).

We investigated different molecular parameters, namely boiling points (**BP**), pK_a and viscosity of organic compounds. We provide here as an example regression models for **BP** of fluoroalkanes. L_1-regularized approaches (**LASSO, LARS**) give a possibility to obtain simplified sets of

descriptors. Corresponding equations have the following form:

LAD: $BP = -416.58 + 5.66 \cdot IAC + 259.29 \cdot HNar \quad R^2 = 0.87, Q^2 = 0.84$ (2)

OLS: $BP = -396.92 + 5.81 \cdot IAC + 243.2 \cdot HNar \quad R^2 = 0.87, Q^2 = 0.85$ (3)

Where IAC and HNar – molecular descriptors which are total information index on atomic composition and Narumi harmonic topological index, respectively. Predictive ability of the alternative regressions obtained in **PCR**, **OLS** and **PLS** is presented in the Fig. 1.

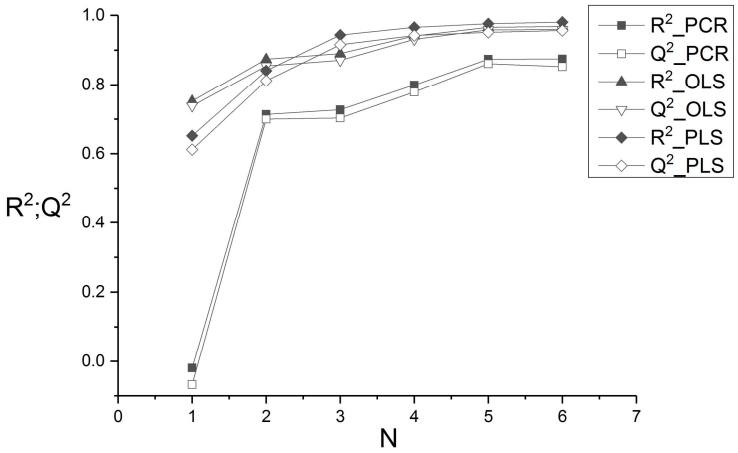

Fig. 1. Comparison of determination coefficients (R^2) and obtained by leave-one-out procedure (Q^2) which were calculated in PCR, PLS and OLS for BP of fluoroalkanes. N – number of regression parameters.

Also we found that the L_1-regularization can be useful in quantum chemistry. Especially for accurate (and computationally demanding) *coupled cluster* with *singles*

and doubles (**CCSD**) and *triples* (**CCSDT**) methods L_1-regularization has been proposed by us [1]. Obtained approximate sets of solutions were used to calculate potential curves for different molecules in **CCSD** and **CCSDT** approaches. It appeared that such an approach even with the number of amplitudes drastically decreased gives almost identical results to those which were obtained with full CC-methods. For instance, for diatomic F_2 dissociation problem following results of **L_1-CCSD** calculation are obtained (Table 1).

Table 1. Regularization parameter (λ), percent of non-zero amplitudes N_t and non-parallelism of potential curves error (NPE) for dissociation curve F_2

λ	0.001	0.002	0.003	0.005	0.01	0.05	0.08	0.1
N_t, %	68.3	62.2	54.7	49.2	36.5	5.2	0.3	0.1
NPE, 10^{-3} a. u.	1.2	2.4	3.6	5.8	12.6	27.3	17.7	12.0

As could be seen, the non-parallelism errors (**NPE**) between exact and approximate potential curves are rather small even for the case of 50 % of amplitudes reduction.

Also in the present work the possibility of using the L_1-regularization in construction of artificial neural networks has been discussed.

References

1. V. V. Ivanov, M. I. Berdnyk and L. Adamowicz, *Mol. Phys.*, 2017, **115**, 2892.

THE EFFECT OF MULTIPLE NITRATION OF 3-DIAZOINDAZOLE ON ITS DETONATION PROPERTIES

Sergey V. Bondarchuk

Department of Chemistry and Nanomaterials Science, Bohdan Khmelnytsky Cherkasy National University, 18031, Cherkasy, Ukraine,
e-mail: bondchem@cdu.edu.ua

Recently, we have analyzed the Kamlet-Jacobs equations with respect to estimation of the relative errors in calculation of detonation velocity (D, m s^{-1}) and pressure (P, GPa) depending on the accuracy of prediction of crystal density (ρ, g cm^{-3}) and the solid state enthalpy of formation (ΔH_f^0, kJ mol^{-1}) [1]. It has been found that the ρ values provide main contribution in D and P, while the ΔH_f^0 values contribute much less. Meanwhile, 3-diazoindazole (**DIND**) has a promising carbon backbone, which can be nitrated to form powerful novel energetic materials possessing high detonation performance, balanced sensitivity and enhanced environmental safety. Crystal structure of **DIND** is illustrated in Fig. 1a [2]. Our calculation of the **DIND** crystal using PBE/NCP/800 eV approach (the bold values in parentheses) provides a good agreement with the experiment on the lattice parameters (Å and deg) [2].

The calculated density of **DIND** is too low (1.480 g cm^{-3}), therefore, we have performed predictions of the condensed-phase densities for mono- and dinitro derivatives of **DIND** using the Polymorph module of the

Materials Studio 7.0 program suite [3]. The calculations were performed with the COMPASS (Condensed-phase Optimized Molecular Potentials for Atomistic Simulation Studies) *ab initio* force-field [4] for the *P*1 space group. As one can see in Fig. 1b, the mononitro derivatives still demonstrate too low densities to exceed common explosives, like RDX or HMX (1.816 and 1.910 g cm^{-3}, respectively). Doubly nitrated isomers also demonstrate different but a bit higher densities. Except of the 5,7-dinitro derivative, all isomers possess densities higher than that of RDX, while the 4,5-dinitro derivative demonstrates the highest density being higher than that of HMX (Fig. 1b). Thus, the latter is the most favorable candidate for use as an energetic compound.

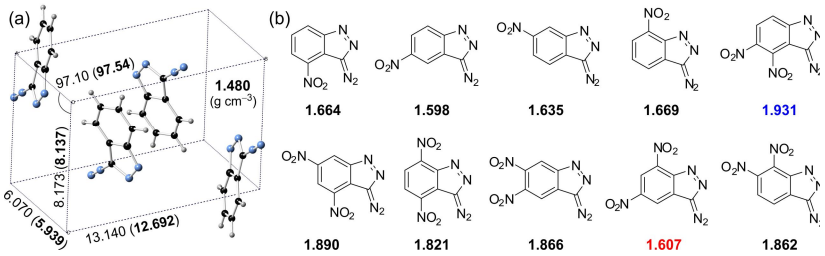

Fig. 1. Crystal packing of **DIND** (a); mono- and dinitro derivatives of **DIND** and their predicted condensed-phase densities (b).

To obtain the ΔH_f^0 values, we have construct three isodesmic reactions (see below) using experimental gas-phase enthalpies (in kJ mol^{-1}) [5] and the calculated enthalpies obtained using one of the most accurate

methods for thermodynamics, namely, CBS-4M [6]. The solid-state enthalpy, calculated using the eq. (1), equals 597.7 kJ mol^{-1}.

$$\Delta H^0_{solid} = \Delta H^0_{gas} + (\frac{E_{solid}}{Z} - E_{gas}) + 2RT \qquad (1)$$

Herein, E_{solid} is the total energy of an asymmetric cell, Z is the number of formula units per asymmetric cell, and E_{gas} is the total energy of a formula unit in the gas phase.

Isodesmic reaction 1

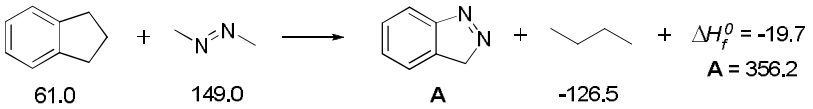

Isodesmic reaction 2

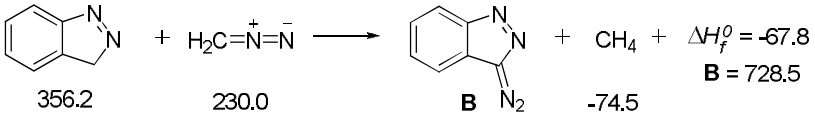

Isodesmic reaction 3

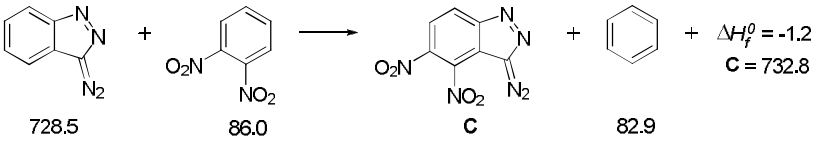

Thus, using the estimated values of ρ and ΔH_f^0, the calculated detonation energy (Q, cal g^{-1}), pressure and velocity for the 4,5-dinitro derivative are 1454.5, 28.8, 7.89, respectively, which is still less than the detonation profile

of RDX and HMX. Thus, insertion of the third and, probably, fourth NO_2 group is needed for exceeding detonation profiles of RDX and HMX; this will be the issue of a separate study.

References

1. С. В. Бондарчук, XIII Всеукраїнська конференція молодих вчених та студентів з актуальних питань хімії, 2-4 травня 2018 р. : тези допов. – Харків, 2018. – С. 27.
2. I. Leban, B. Stanovnik, M. Tisler, *Acta Cryst*., 1978, **B34**, 293.
3. *Materials Studio 7.0*, Accelrys, Inc., San Diego, CA, 2013.
4. H. Sun, *J. Phys. Chem. B,* 1998, **102**, 7338.
5. S. G. Lias, J. E. Bartmess, J. F. Liebman, J. L. Holmes, R. D. Levin, W. G. Mallard, *J. Phys. Chem. Ref. Data,* 1988, **17**, 872.
6. J. W. Ochterski, G. A. Petersson, J. A. Montgomery Jr., *J. Chem. Phys*., 1996, **104**, 2598.

FIRST-PRINCIPLES INVESTIGATIONS OF PhOLEDs' MOLECULAR MATERIALS

Daniel Escudero

CEISAM UMR CNRS 6230, Université de Nantes, 2 rue de la Houssinière, BP 92208, 44322 Nantes Cedex 3, France
e-mail: Daniel.escudero@univ-nantes.fr

Photochemistry is all about competing deactivation mechanisms. The subtle variations of the excited-state structural and energetic factors, that are affected by spin–orbit, and vibronic interactions; as well as by the fine interplay between medium rigidity/polarity and temperature determine the intricate photodeactivation dynamics and the quantum yields of the excited state processes [1].

In this contribution, I present recent studies on quantitative determinations of photochemistry based on the use of state-of-the-art quantum chemical calculations along with excited state decay rate formalism and kinetic modelling. Particularly, we have recently developed general approaches to compute phosphorescent OLED efficiency, [2] and to assess phosphor stability at OLEDs working conditions [3].

References

1. D. Escudero, D. Jacquemin, *Dalton Trans.,* 2015, **44**, 8346.
2. a) X. Zhang, D. Jacquemin, Q. Peng, Z. Shuai, D. Escudero. *J. Phys. Chem. C,* 2018, **122**, 6340; b) D. Escudero, *Chem. Sci.* 2016, **7**, 1262.
3. D. Escudero, *Chem. Sci.,* 2017, **8**, 7844.

CALCULATING SURFACE ELECTROSTATIC POTENTIAL OF MICELLES VIA MOLECULAR DYNAMICS

Vladimir Farafonov, Alexander Lebed, Nikolay Mchedlov-Petrossyan

Department of Physical Chemistry,
V. N. Karazin Kharkiv National University, 61022, Kharkiv, Ukraine,
e-mail: farafonov@karazin.ua

Surface electrostatic potential, Ψ, is a key characteristic of an ionic surfactant micelle. It ultimately affects the distribution of ions in the surrounding solution. The Ψ value is usually estimated via indicator method, namely, if the shift of ionization constant of an acid-base indicator dye in given micellar solution with respect to water is observed. Then, it is converted to Ψ using the so-called HMFF equation, eq. 1. [1].

$$HA_{(m)} \leftrightarrow H^+_{(w)} + A^-_{(m)}\,, \qquad K_a^{app} = a(H^+_{(w)})\,[A^-_{(m)}] \,/\, [HA_{(m)}]$$

$$pK_a^{app} = pK_a^{i} - \frac{\Psi F}{2.303\,RT}\,, \qquad (1)$$

where subscripts m and w mean micelle surface and water phase, respectively, K_a^{app} is the experimentally measured apparent ionization constant of the indicator in micellar solution, pK_a^{i} is the index of the so-called intrinsic ionization constant in that solution, R is the gas constant, T is temperature, F is the Faraday constant.

The term pK_a^{i} includes the effect of all the interactions between the indicator and the micelle, other than the ones

of kind “ion-ion”. The difficulty of the method consists in determining the pK_a^i value for the employed indicator in the solution of interest. Usually, it is approximated with the value of the indicator in some non-ionic micelles, where Ψ = 0. However, this approximation leads to significant spread in Ψ values obtained for the micelles of the same kind by means of different indications.

We propose an approach forcomputing Ψ on the basis of molecular dynamics simulations. It lies in the framework of the indicator method but does not require the pK_a^i value. Instead, the HMFF equation is rewritten in the form of free energies of deprotonation of the indicator (eq. 2), and the contributions of various interactions between the indicator molecule and micelle are directly discriminated using eq. 3. The value of ion-ion contribution is then extracted and converted to Ψ via eq. 4.

$$\Delta G = 2.303RT\mathrm{p}K; \qquad \Delta G_{deprot} = \Delta G_{non-(ion-ion)} - \Psi F \tag{2}$$

$$\begin{aligned}\Delta G_{deprot} &= \Delta G_{ion-ion} + \Delta G_{ion-dipole} + \Delta G_{dipole-ion} + \Delta G_{dipole-dipole} + \Delta G_{van-der-Waals} \\ &= az_iz_m + bz_i + cz_m + d = az_iz_m + \Delta G_{non-(ion-ion)}\end{aligned} \tag{3}$$

$$a = \frac{\partial^2 \Delta G_{deprot}}{\partial z_i \partial z_m}; \qquad az_iz_m = -\Psi F; \qquad \Psi = -\frac{az_iz_m}{F}, \tag{4}$$

where ΔG_{deprot} is the free energy of deprotonation of the indicator in micelle, z_i is the charge of its ionized form, z_m is the charge of micelle (without counter-ions), a, b, c, d are coefficients.

ΔG_{deprot} of the indicator molecule located in micelle is computed via thermodynamic integration algorithm: a series of MD simulations with values of parameter λ clamped in interval [0; 1] is performed, where the limiting values of λ correspond to the protonated and deprotonated forms of the indicator, respectively [2]. Initially, the charge of the deprotonated form equals z_i^0 (e.g. -1 for A^-), and the micelle charge equals z_m^0 (e.g. +80 for a cationic micelle, composed of 80 surfactant ions). However, the computation of ΔG_{deprot} is repeated, taking several $z_i = z_i^0 + \Delta z_i$ and $z_m = z_m^0 + \Delta z_m$.This means that small extra charge is added and distributed uniformly over the indicator molecule (Δz_i) or the head groups of surfactant ions (Δz_m). The charge of counter-ions is held equal by magnitude to that of surfactant ions. The totality of obtained ΔG values allows perform numerical differentiation in eq. 4 and, thus, find the value of Ψ. The calculations are illustrated at Fig. 1.

We applied the described approach to the indicator 4-*n*-dodecyl-2,6-dinitrophenol in micelles of sodium *n*-dodecyl sulfate and cetyltrimethylammonium bromide. The computed Ψ values equal –108 mV and +106 mV, respectively, and fall in the range of values, obtained in experiments.

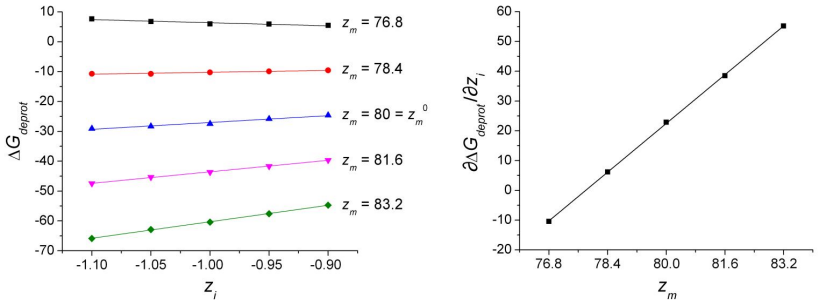

Fig. 1. ΔG_{deprot} values of 4-*n*-dodecyl-2,6-dinitrophenolin cetyltrimethylammonium bromide micelle at different z_i and z_m. The unmodified charges of species equal $z_i^0 = -1$ and $z_m^0 = 80$.

References

1. N. O. Mchedlov-Petrossyan, *Pure Appl. Chem.*, 2008, **80**, 1459.
2. P. V. Klimovich, D. L. Mobley,*J. Comput. Aided Mol. Des.*, 2016, **29** (5), 397.

CREATION OF THE MATERIALS FOR ARTIFICIAL PHOTOSHYNTHESIS

Svitlana Filonenko[1], Natalia Shcherban[2]

[1] Department of Colloid Chemistry,
Max Planck Institute of Colloids and Interfaces,
14476, Potsdam, Germany,
[2] Department of Porous Compounds and Materials,
L.V.Pisarzhevskii Institute of Physical Chemistry of NAS,
03039, Kyiv, Ukraine
e-mail: svitlana.filonenko@mpikg.mpg.de

Modern society operating inevitably leads to increase of the atmosphere pollution by carbon dioxide resulted in the prominent climate change. Main approaches, preventing the pollution, decrease of fossil fuels utilization replacing it with green and sustainable energy sources, and utilization of carbon dioxide for organic molecules creation by artificial photosynthesis. The artificial photosynthesis implementation requires efficient solar energy harvesting and conversion by means of tuning the electronic band structure of semiconductor materials.

For our research we choose carbon nitride as a semiconductor material with wide ability to improve electronic properties by changing its structure and composition [1]. Using hard template method we obtained carbon nitride with ten times increased yield of acetaldehyde in photocatalytic CO_2 reduction comparing to bulk material. By sulphur incorporation into carbon nitride

framework we efficiently disturbed the band structure of the material sufficiently to significantly increase methane and acetaldehyde yields.

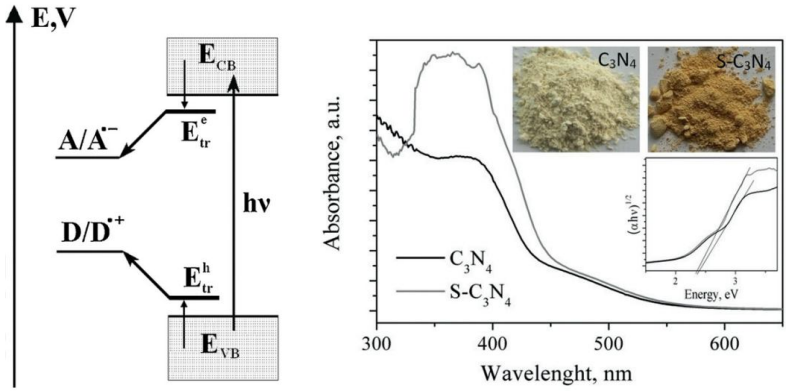

a *b*

Fig. 1 Schematic illustration of electronic processes in photocatalytic systems based on semiconductor particles: A – electron acceptor, D – electron donor, $E^0(A/A\bullet-)$ – reduction potential of electron acceptor, $E^0(D/D\bullet+)$ – oxidation potential of electron donor, E^e_{tr} – potential of surface electron trap, E^h_{tr} – potential of surface hole trap (a); Absorption spectra of carbon nitride samples; insert: spectra in Tauc coordinates for direct transitions (b).

References

1. A. Thomas et al., *J. Mater. Chem.,* 2008, **18** (41), 4893.

INVESTIGATION OF THE MECHANISM OF SILVER NANOPARTICLES FORMATION IN THE REACTION OF Ag^+ WITH PYROCATECHOL VIOLET

Rostislav Galagan, Nataliya Karaush-Karmazin and Boris Minaev

[a]*Department of Chemistry and Nanomaterials Science, Bohdan Khmelnytsky National University, 18031, Cherkasy, Ukraine*

e-mail: karaush22@ukr.net

Pyrocatechol violet (**PV**) is widely used in analytical chemistry as a metal ion indicator from the group of sulfophthalein dyes which represents a tetrabasic acid. This molecule exhibits reducing properties, therefore, interacting with Ag^+ ions it enters an oxidation-reduction reaction. Thus, the study of this interaction should be of interest.

In this paper we have studied the mechanism of oxidation of pyrocatechol violet by Ag^+ ions in alkaline medium which is accompanied by the Ag-nanocluster formation which is in constant contact with the reducing molecule. In general, this system can be considered as a galvanic element, in which the molecule itself acts as an anode and the cathode is a growing metal cluster. In this case, the electric current flows from the **PV** molecule to the metal cluster; the reaction center is a **PV** complex with Ag^+ ion.

The following electrochemical mechanism is proposed for this reaction:

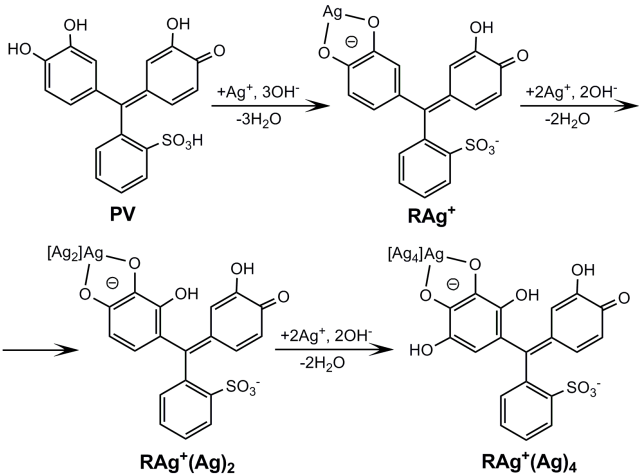

Scheme 1. The proposed mechanism of action of a Ag^+ ion with PV dye in alkaline medium (R – **PV** fragment).

We have also studied a series of UV-visible absorption spectra for the free **PV** and **$RAg^+(Ag)_n$** complexes obtained by partial oxidation of the PV dye. The stoichiometry of these oxidation reactions was studied for the different molar ratios Ag^+ : PV (r_{Ag}) and OH^- : PV (r_{OH}) 1:1, 1:3 and 1:5, respectively. The absorption spectra for the Ag-containing complexes show a strong absorption in the range of 470–350 nm with a new maximum at 400 nm. However, as is shown in Fig. 1, in the **PV** absorption spectrum, we do not observe a clearly pronounced maximum in this range (alkaline medium). It should be noted that the **$RAg^+(Ag)_n$** spectra demonstrate an increase in intensity with an increase in the number of silver

nanoparticles. The reason for this absorption is plasmon resonance in nanoparticles [1].

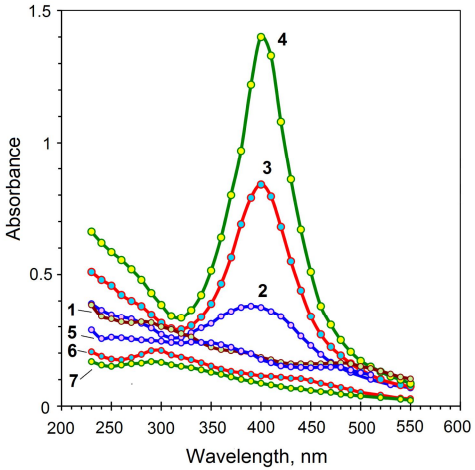

Fig. 1. Experimental UV–vis spectra of the studied species: **1** – for the free **PV** dye, **2** – for the **RAg⁺** system in molar ratio 1:1, **3** – for the **RAg⁺(Ag)₂** (1:3), **4** – for the **RAg⁺(Ag)₄** (1:5), **5** – after silver deposition from the **RAg⁺** system (**2**) by 1 M KCl solution, **6** – after silver deposition from the **RAg⁺(Ag)₂** system (**3**), **7** – after silver deposition from the **RAg⁺(Ag)₄** system (**4**).

Further destroy of the **RAg⁺(Ag)ₙ** systems by 1 M KCl solution leads to the release of all silver in solution. The absorption spectra for solutions after destroy of the **RAg⁺(Ag)ₙ** systems are very similar to the spectrum of the initial **PV** dye.

References

1. C. Noguez, *J. Phys. Chem. C*, 2007, **111** (10), 3806.

FROM (AT)3 AND (GC)3 DNA MINI-HELIXES TO DICKERSON DODECAMER: RESULTS OF RECENT DENSITY FUNCTIONAL THEORY CALCULATIONS

Leonid Gorb

Institute of Molecular Biology and Genetics, NAS Ukraine, 150, Zabolotnogo Str., Kyiv, Ukraine, 03143.
e-mail: leonid.gorb@gmail.com

We present the results of the first comprehensive DFT study of the following DNA minihelixes: (AT)3, (GC)3, (AT)5, (GC)5 and Dickerson dodecamer immersed in vacuum or in water bulk (CPCM model of continuum type). The results are presented in the form of the analysis of geometrical parameters of such DNA building blocks as DNA-bases, nucleosides and nucleotides, and the type of specific hydration of minor and major DNA groves. Also, the stability of Dickerson dodecamer, that contains 'rare' tautomeric forms, is compared with the stability of a conical dodecamer. The comparison of obtained data with the results related to different DNA building blocks (i.e. DNA bases, nucleotides. DNA mini-helixes, etc.) is presented. The optimization of the geometry has been performed at DFT/B97-D3 level augmented by def2-SVP basis set [1].

References

1. R. Wing, H. Drew, T. Takano, C. Broka, S. Tanaka, K. Itakura, R. E. Dickerson, *Nature,* 1980, **287**, 755–758.

2. T. A. Zubatiuk, O. V. Shishkin, L. Gorb, D. M. Hovorun, J. Leszczynski, *Phys. Chem. Chem. Phys.,* 2013, **15** (41), 18155–18166.
3. T. A. Zubatiuk, M. A. Kukuev, A. S. Korolyova, L. Gorb, A. Nyporko, D. Hovorun, J. Leszczynski, *J. Phys. Chem. B*, 2015, **119** (40), 12741–12749.
4. T. A. Zubatiuk, O. Shishkin, L. Gorb, D. Hovorun, J. Leszczynski, *J. Phys. Chem. B*, 2015, **119** (2), 381–391.

DESIGN AND PHOTONICS OF LIGHT ENERGY CONVERTERS BASED ON POLYMETHINE DYES

Alexander Ishchenko

Institute of Organic Chemistry, National Academy of Sciences of Ukraine, 02660, Kyiv, Ukraine
e-mail: al.al.ishchenko@gmail.com

Polymethine dyes are unique converters of light energy. Therefore widely used in various fields of science and technology. Ways to structural modification of the dye molecules, allowing them to smoothly change the electronic structure from the neutral polyene up polymethines and charged polyene demonstrated. Features of photonics of these electronic structures using modern ab initio quantum chemical and spectroscopic methods considered.

Problems creating photochemically stable dyes absorb light intensively in the near-infrared spectral range (800–1700 nm) were analyzed. Structure and properties of the dyes with record Stokes shifts was discussed. Factors contributing to these changes are analyzed. Ways of Stokes shifts increasing were considered.

Posibility of change of the fluorescence quantum yields of 10^{-3} to 1 in polymethines shown. The main nonradiative processes in their molecules are discussed.

Unusual effects of cationic polymethines solvatofluorohromism considered. We found that in contrast to the absorption, in fluorescence is observed an excellent correlation between the maxima of the bands and

the one-parameter function of the universal interactions, despite the fact that the dyes in the excited state as well as in the ground state have a system of strongly alternating charges.

The possibility of creating merocyanines, which have not only record solvatochromism, but also a wide range of changes in the fluorescence quantum yield (from 2 to 97%) depending on the polarity of the medium, is shown. Such dyes are promising for studying the polarity of biomembranes.

Photonics of dyes with two chromophores considered.

It was discussed: the enhancing and quenching the luminescence of polymethines in the low-polarity media, including polymer matrices; anomalously high hypsochromic (100–150 nm) and bathochromic (200–250 nm) shifts of the dyes in these media; the role of the counterion in the deactivation of the excited states polymethines.

Self-organized nanostructure photonics - J-aggregates of dyes discussed.

Intramolecular and intermolecular electron phototransfer in dyes and systems dye – doped photoconductive polymer is considered.

Light energy converters based on polymethine dyes for quantum electronics, nonlinear optics, phototermoplastic holography, photovoltaic and electroluminescence are analyzed.

HIGH-EFFICIENCY WOLED BASED ON DOUBLE EXCIPLEX EMISSION

Khrystyna Ivaniuk[a], Ivan Duplaik[a], Ihor Helzhynskyy[a], Pavlo Stakhira[a], Xaofen Tan[b], Dmytro Volyniuk[b], Juozas V. Grazulevicius[b]

[a]*Lviv Polytechnic National University,*
S. Bandera 12, 79013 Lviv, Ukraine
[b]*Kaunas University of Technology,*
K. Barsausko Str. 59, LT-51423, Kaunas, Lithuania
e-mail: hrustunad@gmail.com

White organic light-emitting diodes WOLEDs have attracted intense research interest due to their wide applications in full-color displays with color filters, backlighting for liquid crystal displays, and lighting sources. The WOLED light emitting radiation is a result of superposition of blue and yellow-green and red electroluminescence of the singlet/triplet exciton nature.

Organic light-emitting diodes (OLEDs) based on thermally activated delayed fluorescence (TADF) emitters are promising devices for display and illumination technologies. Such WOLEDs in which TADF mechanism takes place can be constructed from the donor-acceptor or ambipolar semiconductors. These TADF-based OLED systems usually demonstrate very high internal quantum efficiency equal about 100%. Moreover, such kind of OLEDs are characterized by low values of initial voltage and very high power efficiency [2, 3].

High quality white electroluminescence in WOLED is realized in the work due to the mixing of two colors. For the development of white electroluminescence device as emitters, use of a blue and yellow-green emitter of the exciplex type (TADF) (Fig. 1.).

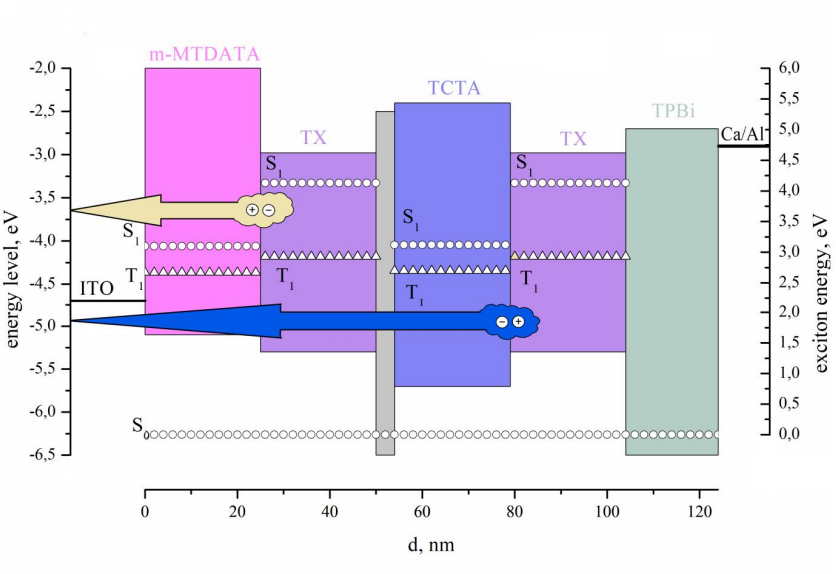

Fig. 1. Schematic energy level diagram WOLED device.

References

1. C. Groves *Nat. Mater*. 2013, **12**, 597.
2. D. Chen, K. Liu, L. Gan, M. Liu, K. Gao, G. Xie *Adv. Mater.* 2016, **28**, 6758.
3. K. Goushi, K. Yoshida, K. Sato, C. Adachi *Nat. Photon.,* 2012, **6**, 253.

PREPARATION OF ELECTROCATALYSTS ON THE BASIS OF COPPER (II) FERRITE

Nina Ivanova, Zeinulla Muldakhmetov, Elena Soboleva, Yakha Visurkhanova

Institute of Organic Synthesis and Chemistry of Coal of Kazakhstan Republic, 100008, Karaganda, Kazakhstan
e-mail: nmiva@mail.ru

Materials based on metal ferrites are widely used in instrument-making, radio electronics, electrical industry, in catalysis and other fields of science and technology. Ferrites of transition metals (Co, Ni, Cu, Zn) and their mixed compositions are most often used in catalysis. In addition, their magnetic properties make it easy to remove them from the reaction system. The reduction of transition metal ferrites is carried out in order to obtain both individual metals (one of which is iron) and their alloys, also used as catalysts.

In this paper, we present the results of studies on the electrochemical reduction of copper ferrites synthesized in the presence of water-soluble polymers (polyvinylpyrrolidone, polyvinyl alcohol, polyethylene glycol) and thermally treated at 500, 700, 900 ^{o}C, and also their manifestation of electrocatalytic properties in the electrohydrogenation of acetophenone, as a model compound.

Samples of copper ferrite $CuFe_2O_4$ were prepared by co-precipitation from a mixture of aqueous solutions of

copper (II) nitrate and ferric chloride (molar ratio 1:2) with the addition of polymer by sodium hydroxide and following thermal treatment (TT). The structure and morphological features of the obtained copper ferrite samples were studied by means of X-ray diffraction (XRD) analysis and electron microscopy.

According to XRD data, it was established that the nature of polymer added to the reaction medium during their preparation, and TT temperature exert some influence on the structure of synthesized copper ferrite samples.

The effect of TT temperature of $CuFe_2O_4$ samples synthesized without polymer additives, before their application in the electrochemical process, is manifested in an increase of copper ferrite crystalline phases content and their crystallinity with increasing temperature. The phase constitutions of $CuFe_2O_4$ + PVP (*1*) and $CuFe_2O_4$+ PEG (*2*) samples thermally treated at the same temperatures practically do not differ from the $CuFe_2O_4$ samples without the polymer, except for the appearance of crystalline phases of hematite (Fe_2O_3) in samples (*2*) and reduced copper (Cu^0) in a small amount in samples (*1*). In comparison with copper ferrite without polymers,the most noticeable differences in the structure are in $CuFe_2O_4$ + PVA (*3*) samples, which already contain copper or/and iron crystalline phases: Cu^0 (500 ^oC), Cu^0<Fe^0 (700 ^oC) after thermal treatment (Fig. 1, *a* and *c*) and $Cu^o \geq Fe^0$ with a decrease in the copper ferrite content (900 °C).

In the compositions of $CuFe_2O_4$ samples (without polymers) after their use in the electrohydrogenation of acetophenone, crystalline phases of reduced copper and iron appear: $Cu^0 > Fe^0$ (500 °C); $Cu^o \leq Fe^0$ (700 °C) (Fig.1, *b*) and $Cu^0 < Fe^0$ (900 °C). Copper (II) and iron (III) cations in different ratios are reduced from copper ferrite, which has passed through the thermal treatment at various temperatures.

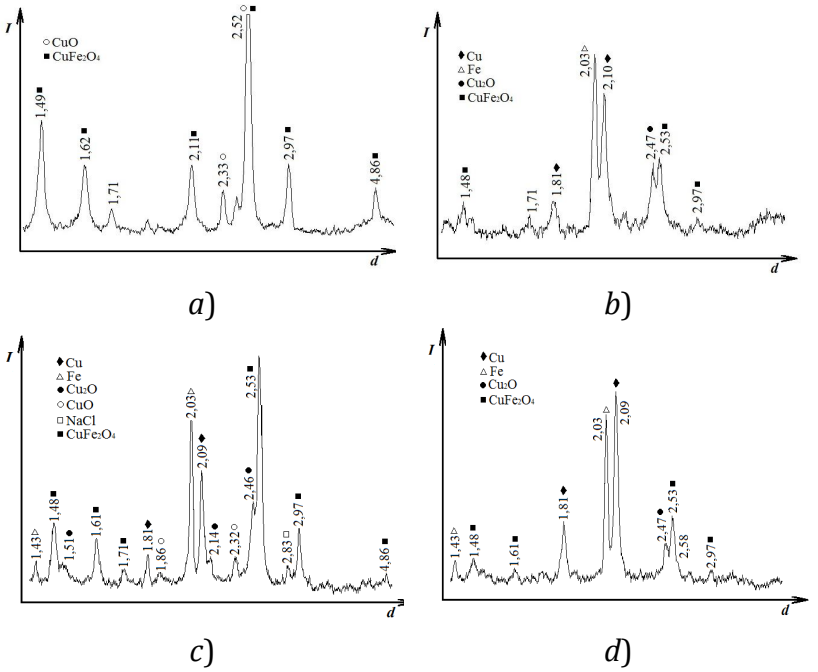

Fig. 1. XRD patterns for $CuFe_2O_4$ (700 °C) and $CuFe_2O_4$ + PVA (700 °C) before (*a, c*) and after (*b, d*) electrocatalytic hydrogenation of acetophenone.

Similar ratios of the crystalline phases of the reduced metals are observed on the X-ray patterns of the samples with polymers *1* and *2* after electrocatalytic hydrogenation of acetophenone. In copper ferrite sample with PVA addition treated at 500 °C, the copper content increases and reduced iron appears, but Cu^0>> Fe^0. Heat treatment of this sample at 700 °C leads to an increase in the content of iron electrochemically reduced (Fig. 1, *d*), and in the $CuFe_2O_4$ + PVA (900 °C) sample, their amounts are equalized: $Cu^0 = Fe^0$.

From electrochemically reduced metals, their micro- and nanoparticles are formed, on the surface of which electrocatalytic hydrogenation of acetophenone is carried out. The main hydrogenation product is methylphenylcarbinol, a known fragrant substance. The electrocatalytic activity of the forming metal or alloy particles depends on their relative content determined by the thermal treatment temperature and the nature of polymer added in reaction medium. The rate of acetophenonehydrogenation in the aqueous alcoholic-alkaline mediumon the catalysts increases by two to six times compared with its electrochemical reduction on the non-activated copper cathode. Acetophenone conversion reaches 100% using copper ferrite samples obtained without polymers and with PVA addition.

MOLECULAR MODELLING AS A CUTTING EDGE TOOL FOR UNDERSTANDING OF THE RTILs BASED ION-MOLECULAR SYSTEMS

Oleg Kalugin

Department of Inorganic Chemistry,
V.N. Karazin Kharkiv National University, 61022, Kharkiv, Ukraine,
e-mail: onkalugin@gmail.com

Room temperature ionic liquids (RTILs) have already found an impressive number of applications due to the versatility of their properties which are determined by their composition. In case of electrochemical application of the RTILs the diversity of credible systems can also be expanded by combining RTILs with dipolar aprotic solvents such as acetonitrile (AN), propylene carbonate (PC) and γ-butyrolactone (γ-BL). The majority of the practically important macroscopic properties of these mixtures is modulated by structure and particle dynamics at microscopic level.

In this contribution we report the results of combined investigation of the set of imidazolium-based RTILs and their mixture with AN, PC and γ-BL by using multitechnique approach including conductometry, NMR and Raman spectroscopy, quasi-elastic neutron scattering (QENS).

A special attention is paid to understanding interparticle interactions, microscopic structure and particle dynamics at atomic and molecular level by using

quantum chemical calculations and molecular dynamics simulations [1-6].

References

1. V. V. Chaban, Iu. V. Voroshylova, O. N. Kalugin, *Phys. Chem. Chem. Phys.,* 2011, **13**(17), 7910.
2. V. V. Chaban, Iu. V. Voroshylova, O. N. Kalugin, *ECS Transactions*, 2011, **33** (28), 43.
3. V. V. Chaban, Iu. V. Voroshylova, O. N. Kalugin, O. V. Prezhdo, *J. Phys. Chem. B.,* 2012*,* **116**, 77197.
4. B. A. Marekha, O. N. Kalugin, A. Idrissi, *Phys. Chem. Chem. Phys.*, 2015, **17** (26), 16846.
5. B. A. Marekha, V. A. Koverga, E. Chesneau, O. N. Kalugin, T. Takamuku., P. Jedlovszky, A. Idrissi, *J. Phys. Chem. B*, 2016, **120** (22), 5029.
6. O. N. Kalugin, A. V. Riabchunova, Iu. V. Voroshylova, V. V. Chaban, B. A. Marekha, V. A. Koverga, A. Idrissi, Transport Properties and Ion Aggregation in Mixtures of Room Temperature Ionic Liquids with Aprotic Dipolar Solvents. Chapter 5, P. 67–109. In: L. Bulavin, A. Chalyi (eds) *Modern Problems of Molecular Physics*. *Springer Proceedings in Physics*, Springer, Cham, 2018, **197**. https://doi.org/10.1007/978-3-319-61109-9_5

MODIFICATION OF MAC-SPECTROMETER MX-7304A FOR DETERMINATION OF LIQUID COMPOSITION

Yaroslav Korol, Nadiia Storozhuk

Department of Physics, Bohdan Khmelnytsky National University, 18031, Cherkasy, Ukraine,
e-mail: yaking@ukr.net

Modern mass-spectrometry is the most sensitive method for the determination of ecotoxicants during ecological monitoring [1]. In particular, this method is used in studying the state of the hydrosphere, depending on the natural geological processes and human economic activity [2]. One of the main mass-spectrometry tasks is to identify the liquids and determine their composition.

Widespread monopoly mass-spectrometer MX-7304A (made in Sumy company SELMI) is designed to control the residual gases composition of technological volumes of vacuumed equipment [3].

In this paper it is shown that this device can also be used to study the molecular composition of liquids, provided that the specimens are transferred to the gas state by means of a special device. Developed vacuum-thermal system for sample preparation consists of the for-vacuum pump, three-position valve and hermetic capacity with the examined sample (see Fig. 1). The heater, pressure and temperature sensors are forming an electronic control circuit. It maintains the optimum vapor pressure of the test fluid at the inlet of the intake valve of the spectrometer

ionization chamber (about 100 mm Hg). In this case, the sample temperature is maintained in the range 20-100°C.

The proposed modification of the mass-spectrometer MX-7304A also allows us to work with a different volatile solids such as camphor, iodine, naphthalene and etc.

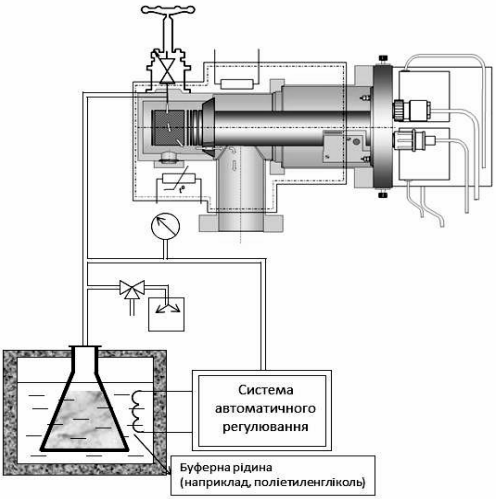

Fig.1. Vacuum scheme of the system to the mass spectrometer MX-7304A.

References

1. A. T. Lebedev *Mass spectrometry for the analysis of environmental objects* (Translation from English under the general editorship of A. T. Lebedev). M: Technosphere, (in Rus.), 2013.
2. A. Bouslimani, et al. Natural product reports, 2014, **31.6**, 718–729.
3. Mass spectrometer MX-7304A. Technical description and instruction manual. JSC «SELMI».

THE RESTRICTION OF INTRAMOLECULAR MOTIONS ORCHANGING RELATIVE POSITION OF THE ENERGY LEVELS OF THE MOLECULES AS A CAUSE FOR AGGREGATION-INDUCED EMISSION

I. V. Korotkova[1], T. V. Sakhno[1], S. Ya. Kuchmy[2]

[1]Poltava State Agrarian Academy, Skovoroda str. 1/3, Poltava 36000, e-mail: sakhno2001@gmail.com, 2irinakorotkova10@gmail.com

[2]L. V. Pysarzhevsky Institute of Physical Chemistry, National Academy of Sciences of Ukraine, Prosp. Nauky, 31, Kyiv 03028, e-mail: kuchmiy@inphyschem-nas.kiev.ua

Most of organic chromophores that are highly fluorescent in solution at low concentration show a drastic decrease of their emission efficiency in the solid state. This is believed to be caused by aggregate formation: in the solid state, the molecules aggregate to form less emissive species such as excimers [1], leading to a reduction in the luminescence efficiency. Aggregation caused quenching has been the thorniest problem in the development of organic light-emitting devices. During the last decades it was founded that some luminogens display the opposite effect: they are non- or weakly emissive in dilute solutions butexhibit bright luminescence upon aggregation. This unique phenomenon is coined as aggregation-induced emission (AIE). Attracted by the prospects of AIE, researchers world wide are engaged in this area and are working on the development of new AIE luminogens, deciphering the underlying mechanism and exploring their

practical applications. Through systematic experimental measurements and theoretical calculations, it has been rationalized that the restrictionof intramolecular motions (RIM), including rotation, vibration, stretching, etc., is highly responsible for the AIE effect [2, 3]. We are interested in extending the AIE luminogens to heterocyclic systems.

Based on our earlier works, which was devoted to the study of the dependence of the spectral-luminescent properties of planar heteroaromatic molecules on the parameters of the external environment (temperature, polarity of the medium, the aggregate state) [4, 5], we believe that the cause of the appearance or disappearance of fluorescence during aggregation is a change in the relative position of the energy levels of the lower electron-excited states of different orbital and spin nature. This especially applies to molecules that do not have rotating fragments.

It was founded that a molecule has an intense fluorescence at following position of energy levels: S_0, $T_{1\pi\pi^*}$, $S_{1\pi\pi^*}$, $T_{2n\pi^*}$, $S_{2n\pi^*}$. However, under the influence of temperature or as a result of aggregation, the inversion of $S_{\pi\pi^*}$ and $T_{n\pi^*}$-levels can occur, which leads to a change in the fluorescence intensity (Scheme 1) [4]. The competitive

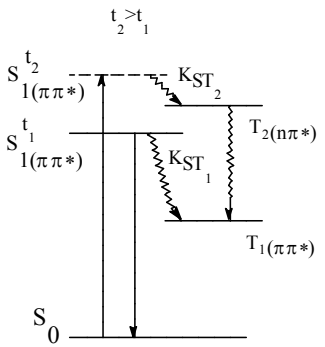

process with the fluorescence was found to be intersystem crossing to the triplet state. The decisive role belongs to the ISC rate constant, which is of the order of 10^8 s^{-1} if the process occurs between states of the same orbital nature ($S_{\pi\pi}$ and $T_{\pi\pi}$), i.e. has one order with a fluorescence constant (10^7 s^{-1}). If the ISC process is performed between electronic states of different orbital nature ($S_{\pi\pi}$ and $T_{n\pi}$), the rate constant is 10^{10} s^{-1}, which leads to almost complete suppression of fluorescence. It should be noted that the value of the ISC rate constant depends on the energy gap between the interacting energy levels.

The origins of increasing the fluorescence intensity in heteroaromatic molecules are supported with the aid of the results of theoretical calculations. It was founded that the effect of temperature as aggregation should be associated with a change in the length of the C=O or C=N-fragments and, correspondingly, a change in the relative position of the energy levels of the lower electronic excited states [5, 6]. So, the quantum-chemical calculations of electronic state energy of acridone molecule versus >C=O bond (left) adequately interpreted the experimental data about

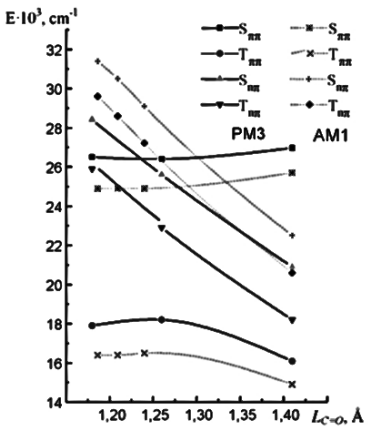

change of relative position of energy levels of acridone molecule in different mediums.

The graphical dependencies of electronic state energy of coumarine versus solvent polarity Kirkwood-Onzager constant confirm the experimental data on the absence of fluorescence of unsubstituted coumarin, since the lowest singlet level of the dye is of nπ-nature(on right). An increase in the solvent polarity is accompanied by a significant increase in the energy of the nπ-levels and, as follows from the data obtained, one should expect the appearance of fluorescence due to inversion of the $S_{n\pi}$ and $S_{\pi\pi}$ levels. Thus, varying the length of the heteroaromatic fragment can influence on the fluorescence efficiency. The numerous investigations carried out allowed making a conclusion about relation of fragment geometry and energy of nπ-levels of heteroaromatic molecules. We believe that the reason for the origin of the AIE effect at the aggregates formation is the change in geometry of molecules (the length of the chromophore fragments), which leads to a change of the relative position of the energy levels of the lowest electronic excited states.

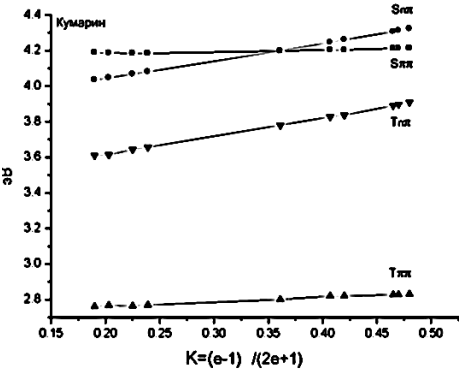

References

1. N. N. Barashkov, T. V. Sakhno, R. N. Nurmukhametov, O. A. Khakhel', *Russ Chem Rev.*, 1993, **62** (6), 539.
2. J. Mei, N. L. Leung, R. T. Kwok, J. W. Lam, B. Z. Tang, *Chem. Rev*., 2015, **115** (21), 11718.
3. V. M. Granchak, T. V. Sakhno, I. V. Korotkova, Yu. E. Sakhno, S. Ya. Kuchmy, *Theor. Exp. Chem.*, 2018, **54** (3), 147.
4. T. V. Sakhno, I. V. Korotkova, O. A. Khakhel', *Functional Materials*, 1996, **3** (4), 502.
5. T. V. Sakhno, I. V. Korotkova, O. A. Khakhel', *Theor. Exp. Chem.*, 1996, **32** (4), 217.
6. T. Novikova, T. Sakhno, I. Korotkova, N. Barashkov, Yu. Sakhno, I. Irgibaeva, *Phys. Chem. Solid State*, 2012, **13** (1), 205.

AB INITIO MD STUDY OF POLARIZATION EFFECTS IN LIQUID ACETONITRILE AND SOLUTION OF LITHIUM ION IN ACETONITRILE

Oleksandr Korsun, Oleg Kalugin

Department of Inorganic Chemistry, Faculty of Chemistry,
V. N. Karazin Kharkiv National University, Kharkiv, Ukraine
e-mail: oleksandr.korsun@gmail.com

Accounting of the polarization effects has a significant meaning for the classical Molecular Dynamics (MD) simulation of the polar molecular liquids, ionic liquids and their mixtures, as well as solutions of the high-polarizing ions in the mentioned solvents. Incorporation of both solvent-solvent polarization and solute-solvent charge transfer in the corresponding MD force field models has considerable impact on the simulation results.

Acetonitrile (AN) is a widely used solvent in the fundamental investigations and applied electrochemistry. Nowadays solutions on the base of AN are commonly used in the Electric Double-Layer Capacitors and Li-ion based Hybrid Supercapacitors [1]. In the present study an *Ab Initio* MD simulation of the self-polarization effect in the liquid AN and charge transfer between the Li^+ ion and surrounded AN molecules in the infinitely diluted solution were performed.

For calculations the plane-wave pseudopotential Density Functional Theory was selected at the validated BLYP&TM/90Ry level of theory with and without the D2 vdW-corrections by Grimme using the CPMD-3.13.2 program. MD trajectories were generated using the Car-

Parrinello approach at the 298 K. Obtained coordinates of the atoms and Wannier centers were analyzed using the TrAVis tool [2].

For the first time it was shown that in the liquid AN averaged partial charge on the hydrogen atoms is negative [3]. Obtained −0.004 and −0.005 values were derived from the total electrostatic potential with and without vdW-corrections, respectively. Computed AN dipole moment distribution functions (Fig. 1) demonstrate asymmetric shift in direction of the higher values for the solution of Li^+ ion with respect to the pure solvent. Given result was treated as the charge transfer within the solvation shell of cation: from the nearest AN molecules to the solvated Li^+ ion.

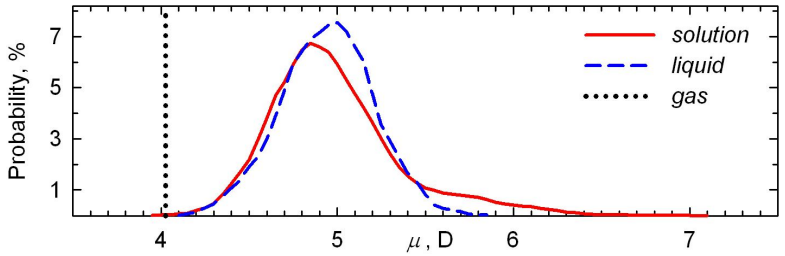

Fig. 1. Distribution functions of the AN molecules dipole moment (μ) in the gas and liquid states, and in solution of the Li^+ ion in AN.

References

1. K. Naoi, S. Ishimoto, J.-i. Miyamoto, W. Naoi, *Energy Environ. Sci.*, 2012, **5**, 9363.
2. M. Brehm, B. Kirchner, *J. Chem. Inf. Model.*, 2011, **51**, 2007.
3. V. A. Koverga, O. M. Korsun, O. N. Kalugin, B. A. Marekha, A. Idrissi, *J. Mol. Liq.*, 2017, **233**, 251.

pH DEPENDENT HYDROGEL SYSTEMS BASED ON POLYESAHARIDES

Oksana Kostyk, Maria Matviychuk,Volodymyr Vostres, Olha Budishevska

Department of Organic Chemistry, Lviv Polytechnic National University, 79013, Lviv, Ukraine,
e-mail: budishevska@gmail.com

In the modern world, the important issue is the creation of new materials that are environmentally safe and biodegradable, not harmful to humans, derived from reproducible, common and in exhaustible sources, economically profitable. Especially interesting for the use in the food, cosmetic and pharmaceutical industries, agriculture and medicine are carbohydrates. The presence of amino groups in the macromolecules of carbohydrates provides such the properties as the ability to complexize with heavy metals and toxic substances, biocompatibility, bactericidality. Such the carbohydrates are chitin and deacetylated chitin – chitosan. However, the most affordable and cheap polysaccharide is starch.

In this work, pH-dependent hydrogels of two types were obtained: using polysaccharides of chitosan (Chit) and sodium alginate (Alg); or aminated starch (St-AR) and Alg and examined their ability to swell, depending on pH of a medium. Hydrogels based on chitosan and sodium alginate (Chit -Alg) were prepared by combining 1% water colloidal solutions of Chit and Alg at different ratios of amino groups at the links of

the Chit and carboxylate groups in Alg. As a cross-linking agent in the formation of the three-dimensional grid of the hydrogel Ca^{2+} ions. It is known that Ca^{2+} ions in aqueous solutions of sodium alginate interact with 10 atoms of oxygen in the blocks of hyaluronic acid in Alg macromolecules. In this case, an intermolecular cell is formed, in the center of which is Ca^{2+}. The nature of these interactions is electrostatic and coordination (donor-acceptor). In this case the three-dimensional mesh of type 2 hydrogel is formed. However, the intermolecular interaction of Chit and Alg through the electrostatic interaction of ammonium groups of chitosan and carboxylate groups of alginate also contributes to the formation of the polymeric grid of the hydrogel.

Aminated starch with ammonium groups (St-AR) was obtained by the interaction of corn starch (St) in an aqueous colloidal solution and an amine reagent (AR). The amine reagent was obtained by reacting epichlorohydrin and triethylamine hydrochloride in the presence of a catalyst. In the formation of hydrogels on the basis of amine starch and sodium alginate (St-AR-Alg), as a crosslinker, calcium carbonate and sorbic acid were used, as in the case of the formation of the hydrogel Chit-Alg. Ca^{2+} ions interact with hyaluronic acid compounds in alginate, at the same time, ammonium groups St-AR electrostatically interact with carboxylate Alg groups. In this case, the three-dimensional mesh of type 2 hydrogel is formed.

It is shown that the dependence of the degree of equilibrium swelling (A_r) of the hydrogels of both the types

(Chit-Alg and St-AR-Alg) from pH of the aqueous medium in the pH range of 1.3 – 12.0 has an extreme character in both the cases. At pH less than 3 the degree of equilibrium swelling of the Chit-Alg and St-AR-Alg hydrogels have the slowest values due to the presence of Alg carboxylate groups. At low pH there is the decrease in the ionization of -C(O)OH groups and the collapse of the carboxylate component. With the pH increase, the degree of equilibrium swelling of the hydrogels of both the types increases to the maximum value.

In the pH range of 5 – 6, the maximum value of A_r has the hydrogel Chit-Alg, and in the range of pH 4 – 6, the hydrogel of St-AR-Alg (depending on the ratio of Alg and the amine-containing component).

With the increase in pH up to 10 – 12 A_r decreases in the case of both the types of the hydrogels. This is due to the presence of an amine-containing component.

At pH 10-12 $-NH_3^+$ turns into $-NH_2$ and decreases the mutual repulsion of macrocations and the amount of solvate water in Chit-Alg.

In the case of hydrogels St-AR-Alg with the pH increase from 6 to 9 also occurs the decrease of the degree of ionization of ammonium groups in macromolecules of aminated starch, and, consequently, the decrease of their solvation and A_r.

The obtained macrohydrogels Chit-Alg and St-AR-Alg can absorb water-soluble dyes from an aqueous medium. Dried and filled with dyes xerogels release them when

swollen in an aqueous medium, depending on pH. The conducted researches allow to offer the received pH-dependent hydrogel systems on the basis of polysaccharides Chit and Alg and St-AR-Alg for the use in cosmetology, at creation of new preparations for care and treatment of skin.

MOLECULAR QUANTUM THEORY ≥ COMPUTATIONAL CHEMISTRY
WHERE DO WE STAND?

Eugene S. Kryachko

Bogolyubov Institute for Theoretical Physics, Kiev 03143 Ukraine
E-mail: eugene.kryachko@gmail.com

"Any headline ending in a question mark
can be answered with the single word *No*."
– journalist's adage
(the Davis-Hinchliffe-Betteridge law)

This work is about the three-stage path that computational chemistry passed from the birth of quantum mechanics that is always referred to the times when the concept of quanta arose and which were described by J. Wheeler in his 1986th paper "How Come the Quantum?" [1] – to the beginning of the 19th century: in Max Planck's work in 1900 to the black-body radiation problem and in Albert Einstein's 1905th paper on the photoelectric effect, – though Ernest Rutherford called the year of 1896 the origin of quantum revolution because in this year A. H. Becquerel in his Paris laboratory discovered the radioactivity.

The second stage falls on the mid-1920s when the early quantum mechanics was profoundly re-conceived by E. Schrödinger, W. Heisenberg, and M. Born, and when in his 1926-year paper "An Undulatory Theory of the Mechanics of Atoms and Molecules" [2], E. Schrödinger

suggested a partial differential equation since then bearing his name – the Schrödinger equation that stands for the mathematical embodiement of quantum mechanics, and actually revived the molecular quantum mechanics.

The third stage, according to E. Bright Wilson [3], refers to the 1926–27 years, when quantum chemistry began: there were four, Heitler, London, Mulliken, and Hellmann [4, 5]. Two-years later P. A. M. Dirac made his famous forecast in the opening paragraph of his 1929-year paper [6]: “The general theory of quantum mechanics is now almost complete... The underlying physical laws necessary for the mathematical theory of a large part of physics and the whole of chemistry are thus completely known, and the difficulty is only that the exact application of these laws leads to equations much too complicated to be soluble. It therefore becomes desirable that approximate practical methods of applying quantum mechanics should be developed, which can lead to an explanation of the main features of complex atomic systems without too much computation.” This marked the revival of computational chemistry with its "computational observations" (a so called "computationism"; see e.g. [7]).

Recent years have witnessed a remarkable surge of interest in quantum mechanics. To date, there has been no experimental evidence that invalidates it. On the contrary, since its inception, quantum mechanics has been verified to extremely high precision and forms the basis of a vast array of new technologies. On the other hand, since the seminal

work [8] by Einstein, Podolsky, and Rosen (EPR) in 1935, mostly known as the EPR paradox, it has been concluded that the description of reality provided by quantum theory is incomplete because it is incompatible with the concept of locality and realism [9]. The latter is also related to the standard theory of measurement in quantum theory that was based on the probabilistic interpretation of quantum mechanics – this fact was mentioned by Wigner [10]. In 1964, Bell [11] derived the famous inequality that was a sort of ``tool" to experimentally discriminate the quantum predictions and local-realist properties and, assuming locality and realism, ``limits the degree to which measurement outcomes on pairs of distant systems may be correlated, if the measurements of one system are carried out with only limited information about the other" [12].

Quantum mechanics is the predecessor of quantum chemistry that may inherit its incompleteness in describing the reality [13]. This work unravels three paradoxical examples of such incompleteness of quantum chemistry. The one is the existence of the He-He bond in the endofullerene $He_2@C_{60}$ [14]. The second is related with the definition of a hydrogen bond [15], and the third with the interpretation of point mutations in the A-T pair of DNA [16]. Herein, we demonstrate the ways of resolving these paradoxes by introducing somewhat implicit definition of a bond.

References

1. J. Wheeler, How come the quantum? New Techniques and Ideas in Quantum Measurement Theory, ed. by D. Greenberger, *Ann. N.Y. Acad. Sci*, 1986, **480**, 304–316.
2. E. Schrödinger, An Undulatory Theory of the Mechanics of Atoms and Molecules, *Phys. Rev.*, 1926, **28**, 1049–1070.
3. E. Bright Wilson, Fifty Years of Quantum Chemistry, *Pure Appl. Chem*., 1976, **47**, 41–47.
4. W. H. E. Schwarz *et al*., Hans G. A. Helmann (1903–1938) Part I. A Pioneer of Quantum Chemistry. Part II. A German Pioneer of Quantum Chemistry in Moscow, *Bunsenmagazin* **1**, 10–21, **2**, 60–70 (1999).
5. S. D. Peyerimhoff, The Development of Computational Chemistry in Germany, In Reviews in Computational Chemistry, Vol. 18, K. B. Lipkowitz and D. B. Boyd, Eds. (Wiley, Hoboken, N.J., 2002), pp. 257–291.
6. P. A. M. Dirac, Quantum Mechanics of Many-Electron Systems, *Proc. R. Soc. Lond Ser. A*, 1929, **123**, 714–733.
7. K. Popper, in Open Questions in Quantum Physics, G. Tarozzi and A. van der Merwe, Eds. (Reidel, Dordrecht, 1985), pp. 395–413.
8. A. Einstein, B. Podolsky, and N. Rosen, Can Quantum-Mechanical Description of Physical Reality Be Considered Complete? *Phys. Rev.*, 1935, **47**, 777–780.
9. D. Deutsch, The Fabric of Reality (The Penguin Press, Allen Lane, 1997).

10. E. P. Wigner, The Problem of Measurement, *Am. J. Phys.*, 1963, **31**, 6–15.
11. J. S. Bell, On the Einstein Podolsky Rosen Paradox, *Physics*, 1964, **1**, 195–200.
12. J. Handsteiner *et al*. Cosmic Bell Test: Measurement Settings from Milky Way Stars, *Phys. Rev. Lett.*, 2017, **118**, 060401.
13. H. Primas, Chemistry, Quantum Mechanics and Reductionism (Springer, Berlin, 1983).
14. T. Yu.Nikolaenko, E. S. Kryachko, and G. A. Dolgonos, On the Existence of He-He Bond in the Endohedral Fullerene $He_2@C_{60}$, *J. Comput. Chem. Special Issue: Quantum Crystallography*, 2018, **39**, 1090–1102.
15. E. Arunan, G. R. Desiraju, R. A. Klein, J. Sadlej, S. Scheiner, I. Alkorta, D. C. Clary, R. H. Crabtree, J. J. Dannenberg, P. Hobza, H. G. Kjaergaard, A. C. Legon, B. Mennucci, D. J. Nesbitt, Definition of The Hydrogen Bond, *Pure Appl. Chem.*, 2011, **83**, 1637–1641.
16. E. S. Kryachko and S. N. Volkov, To The Understanding of The Mechanism of Formation of Point Mutations in DNA, *Doklady Nat. Acad. Sci. Ukraine*, 2018, **7**, 103–112.

THEORETICAL SEARCH FOR ENVIRONMENTALLY FRIENDLY COMBUSTION INHIBITORS

Vitalina Kukueva

State Institution "Institute of environmental geochemistry"
03680, Kiev-142, Av. Palladin Academik, 34a,
e-mail: vitalina.kukueva@gmail.com

It is well known that addition of halogens to flames promotes extinction at least partially through modification of the chemical kinetics. It was shown before that Chlorine atom catalyzed destruction of ozone [1]. The large amount of Chlorine and Bromine containing fire extinguishing substances have been banned as for applications as for production [2]. The search of new environmentally friendly flame inhibitors is actual current scientific task. Improved knowledge of mechanisms by which these agents operate may help in advancing fire suppression strategies. The scope of the theoretical research is limited to chemical suppressants acting mainly on the hydrogen flames. It is well known that the flame propagation mechanism on hydrogen-air flames at the pressure above one atmosphere the clue role plays hyper equilibrium concentration atoms and radicals connecting with chain brunching reactions. Addition a few inhibitor amount, which able to catch (scavenge) the radicals can significant to reduce combustion speed [3].

The fire suppressant powders could stop fire by chemical way rather than physical. The inhibition action

consists in the scavenging activity, when chemical substances destruction products capture the active centers of flame (ACP) to form molecules or stabile intermediates [3]. The surface recombination ACP along with chain abrupt are also the important energy channel from reactive gases, because the energy radiate due to heterogeneous radicals ruin could be absorb by solid powder particles.

There are some mechanisms for fire suppression action of phosphorus containing compounds. So, in the Twarowski papers [4] has been shown that the main inhibiting components of phosphorus containing mixtures are phosphorus oxides: $H^{\bullet} + PO_2^{\bullet} \rightarrow HOPO^{\bullet}$; $H^{\bullet} + HOPO^{\bullet} \rightarrow H_2 + PO_2^{\bullet}$; $OH^{\bullet} + H_2 \rightarrow H_2O + H^{\bullet}$.

These reactions include $PO_2^{\bullet}$ and $HOPO^{\bullet}$ radicals as a catalysts, because there are the same amount of them after reaction. First two of the reactions are catalyzing of $H^{\bullet}$ recombination to form H_2, as far as third one forms H_2O. Our calculations had shown the important role in the inhibition cycle has also $PO^{\bullet} + O^{\bullet} = PO_2^{\bullet}$ reaction. It was proposed to use dispersed silica as catalytic support for inhibiting phosphorus containing particles [5].

The quantum-chemical calculations by the *ab initio* method in the 6-311G(d,p) basis set have been provided to research the chemical way to destruct of inorganic phosphorus containing particles (Table 1). This method is founded effective for obtaining of different chemical structure intermediates. Such structures have high thermal stability and didn't move quickly to be bounded by strong

chemical bounds and this fact opens possibility for the study their reactivity and destruction pathways. For the next stage the collision complexes between destruction products and active centers of flame ($H^{\cdot}$, $OH^{\cdot}$, $O^{\cdot}$) have been calculated to research scavenging effectiveness of these substances. The relative stability of the short living complexes has been determined by the comparative analysis of bind lengths and energies.

Table 1. *Ab initio* calculation in the 6-311G(d,p) basis set of flame inhibition cycle reactions with $PO^{\bullet}$ and $PO_2^{\bullet}$ radicals participation

No	Elementary reactions	Interaction energy, E kcal/mol
1	$PO^{\bullet} + O^{\bullet} = PO_2^{\bullet}$	25.1
2	$PO^{\bullet} + OH^{\bullet} = HOPO$	50.2
3	$PO^{\bullet} + H^{\bullet} = HPO^{\bullet}$	37.6
4	$PO_2^{\bullet} + OH^{\bullet} = HOPO_2$	18.8
5	$PO_2^{\bullet} + H^{\bullet} = HOPO$	81.5
6	$HOPO + H^{\bullet} = PO_2^{\bullet} + H_2$	6.3
7	$HOPO + OH^{\bullet} = PO_2^{\bullet} + H_2O$	6.5

The calculation results (Table 1) had shown, that the most probable 1, 3, 4, 6, 7 reactions. Besides, $PO^{\bullet}$, $PO_2^{\bullet}$, HOPO particles are the most active components scavenging active centers of flame, that coincide with Twarowski experiments [3]. Therefore these radicals play the main role in inhibition at the phosphorus containing powders application. It was proved [5] that $PO^{\bullet}$ and $PO_2^{\bullet}$ radicals destruction energy from the silica surface by three times

less than from the $(NH_4)_3PO_4$ molecules. So, it could be used as catalytic support for increasing of flame inhibitors effectiveness.

References

1. M. J. Molina, F. S. Rowlard, *Nature*, 1974, **24**, 810.
2. http://www.ciesin.org/TG/PI/POLICY/montpro.html.
3. A. Twarowski, *Combustion and Flame*, 1996, **105**, 407.
4. V. Namrata, J. Siow, N. Lawendeau, *Combustion and Flame*, 2001, **126**, 1393.
5. V. V. Kukueva, V. M. Bogatyrev, V. V. Lobnov, *Pat. №39937 Ukraine*, A62D 1/00. Publ.25.03.2009; Bul. N 6. – 4 p.

QUANTUM-CHEMICAL MODELING FOR FORMATION OF SILVER CLUSTERS, STABILIZED BY PRODUCTS OF ALIZARIN OXIDATION

Valentina Litvin[a], Boris Minaev[a], Roger Njoh[b], Tetyana Petrova[a], Iryna Kalashnyk[a]

[a]*Department of Chemistry and Nanomaterials Science, Bohdan Khmelnytsky National University, 18031, Cherkasy, Ukraine,*

[b]*Faculty of Pharmacy, Department of Toxicology, Near East University, 99138 Nicosia, North Cyprus*

e-mail: litvin_valentina@ukr.net

The interaction of Ag^+ ion with alizarin in an alkaline medium leads to the formation of silver nanoclusters system whose particle size, according to X-ray diffraction data, is about 20 nm. Since the oxidation of alizarin (Alis) is accompanied by the consumption of OH-ions, it seems reasonable to propose the hydroxylation of aromatic rings of the alizarin molecule by the Elbs type [1]. The stoichiometry of the process was studied by the molar ratio method in a series of experiments in which the ratios Ag^+:Alis (r_{Ag}) and OH^-:Alis (r_{OH}) varied. In the presence of alizarin, no precipitation of silver oxide is observed, which apparently forms a microphase. On the basis of experimental data, a mechanism for the formation of silver nanoparticles was proposed. To confirm the proposed mechanism, calculations were made of the primary clusters of silver combined with the alizarin molecule.

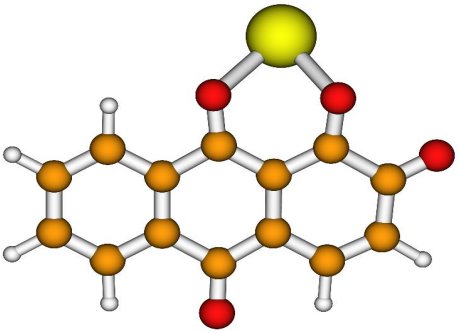

Fig. 1. The singlet state of the complex $[Ag(Alis)]^-$.

Since the final nanoparticle contains about 500 silver atoms and the crystal structure in it is analogous to that of a massive metal, the concept of spin for an electron gas loses its meaning (any spin states are quasi-degenerate), then the growth of the nanoparticle, starting from the primary structures, is not forbidden on the back. In this case, the change in spin in the first stage (the S-T transition for the complex given in Fig. 1) seems to be of fundamental importance, since it represents a qualitative transition from exclusively diamagnetic initial structures (alizarin, silver ions, hydroxide ions) to cluster formations of pseudometallic type.

References

1. M. V. Canamares, P. Sevilla, S. Sanchez-Cortes, J. V. Garcia-Ramos, *Biopolymers* , 2006, **82**, 405.

THE NEW DEPENDENCIES IN CHRONOPOTENTIOMETRY OF ALTERNATING CURRENT

Olena Lut, Tatyana Petrova and Rostislav Galagan

Department of Chemistry and Nanomaterials Science, Bohdan Khmelnytsky National University, 18031, Cherkasy, Ukraine

e-mail: lutlen@ukr.net

The use of alternating current at a frequency of 50 Hz in chronopotentiometry was first described by Ya. Heyrovsky [1], which introduced the dependence $\mathrm{d}E/\mathrm{d}t = f(E)$. The reciprocal derivative variant $\mathrm{d}t/\mathrm{d}E = f(E)$ by D. Jagner was proposed [2]. When multiplying the signal by the average value of the current in the corresponding interval of time, we obtain the value of the differential capacitance of the electrode $\mathrm{d}q/\mathrm{d}E$, which is expressed of the equation: (1)

$$C_d = \frac{\Delta q}{\Delta E} = \frac{\Delta t}{\Delta E} \cdot \bar{I}_{dis} = \frac{\Delta t}{\Delta E} \cdot I_a \cdot \sin(\omega \cdot (t_i + t_{i+1})/2 + \varphi). \quad (1)$$

In Fig. 1*a* shows the dependencies C_d vs E and $\mathrm{d}E/\mathrm{d}t$ vs E for 0.01 M camphore solution. The separation of the faradic component of the total capacity out using a MathCAD script was carried (see Fig. 1*b*). This achieved by subtracting the values of C_d for the supporting electrolite from the corresponding values for the solution of depolarizer at the corresponding potentials. The advantage of the proposed dependence is that the peaks of processes

may have a characteristic and reproducible structuring, which in our opinion opens up opportunities for studying the mechanisms of rapid electrochemical reactions.

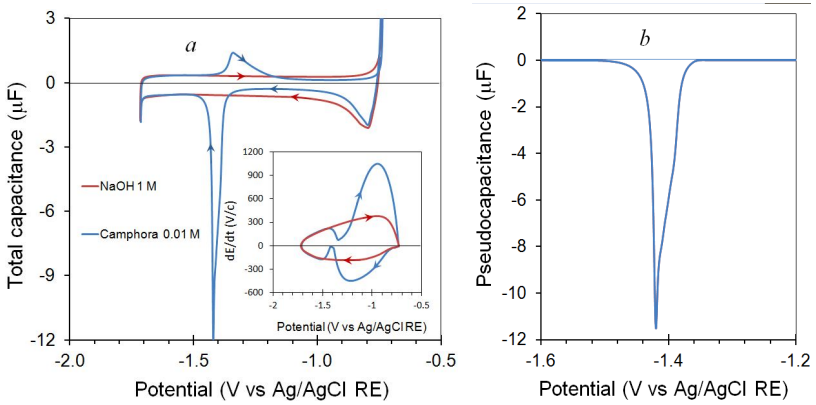

Fig. 1. Dependencies C_d vs E and dE/dt vs E (a) for camphora; faradic component of C_d (b).

References

1. J. Heyrovský, *Anal. Chim. Acta*, 1948, **2**, 533–541.
2. D. Jagner, *Trends Anal. Chem.*, 1983, **2**, *53–56.*

ANALYSIS OF IR AND RAMAN VIBRATIONAL SPECTRA FOR THE HIGHLY-SYMMETRICAL OCTATHIA[8]CIRCULENE

Valentina Minaeva[a], Nataliya Karaush-Karmazin[a], Boris Minaev[a], Gleb Baryshnikov[a,b], Hans Ågren[b]

[a] *Department of Chemistry and Nanomaterials Science, Bohdan Khmelnytsky National University, 18031, Cherkasy, Ukraine*
e-mail: minaeva@cdu.edu.ua

[b] *Theoretical Chemistry, School of Biotechnology, Royal Institute of Technology, SE-10691 Stockholm, Sweden*

Octathia[8]circulene (**8S**) (Fig. 1(a)) is the unique representative of organic macroheterocycles which contain inner planar cyclooctatetraene (COT) core.

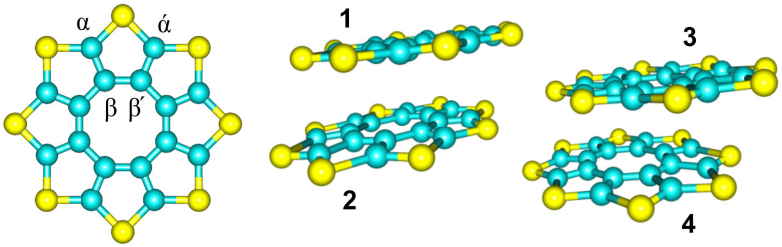

(*a*) (*b*)

Fig. 1. The optimized structures of octathia[8]circulene (*a*) and tetramer (*b*).

The octathia[8]circulene was synthesized in 2006 by Nenajdenko et. al. through the vacuum pyrolysis of the corresponding cyclic polythiol [1]. Compound **8S** was found to be absolutely planar system according to X-ray

diffraction analysis being in a good agreement with the Wynberg-Dopper's structural model [2]. The main feature of this compound is a high molecular symmetry defined by the D_{8h} point group which is responsible for its unique spectral properties. The most clear manifestation of the molecular symmetry role is exhibited in vibrational IR and Raman spectra of compound (**8S**) detected for the first time by Bukalov et. al [3]. They have also performed the quantum-chemical explanation of experimental data, but many vibrational features (like symmetry assignments of some normal modes, Davydov splitting phenomenon in Raman spectra and analysis of symmetry-forbidden modes) remain unexplained and require more detailed theoretical study. Thus, we have performed an analysis of IR and Raman vibrational spectra for this highly-symmetrical hetero[8]circulene accounting for the structural peculiarities on the ground of density functional theory (DFT).

Molecular structure of the studied octathia[8]circulene was optimized at the B3LYP/6–31+G(d,p) [4–6] DFT level [7, 8] with the control of possible symmetry constrains using the Gaussian 16 package [9]. Vibrational frequencies with the corresponding IR intensities and Raman activities were calculated for the optimized geometry by the same DFT method. The calculated vibrational frequencies were calibrated with the scaling factors 0.987 for the whole observed region of the spectrum 1600–100 cm^{-1}. Raman

activities (S_i) were recalculated into the relative Raman intensities (I_i) [10]. The calculated vibrational IR and Raman spectra were plotted using the SWizard 4.6 program [11] using the Lorenz-type distribution function (the lines' half-width is 2 cm^{-1}).

The calculated normal vibration (NV) frequencies of the **8S** molecule do not afford to make clear assignment of many experimental weak IR and Raman bands [3]. Some of these bands are not predicted by our DFT calculations (with different basis sets) in agreement with Bukalov's DFT results (where PBE functional with the SBK and 6-311G* basis sets were used [3]). Thus, the reason for such disagreement between the measured and calculated vibrational spectra for molecule **8S** could be determined by the intermolecular perturbations in the lattice. In order to explain the occurrence of new weak lines and their splitting in experimental vibrational IR and Raman spectra we have simulated the crystal packing by calculation of dimer and tetramer structures of compound **8S**. We need to use smaller basis set (6-31G(d)) since the tetramer calculation (96 atoms) in the large basis set is impossible. We also introduce the dispersion correction for account of intermolecular interactions (B3LYP/GD2). The started atomic coordinates before geometry optimization in tetramer were obtained from X-ray diffraction analysis of the red crystal of octathia[8]circulene [3]. In order to compare the calculated results for tetramer and for a single molecule we have performed additional optimization and

vibrational IR and Raman spectra DFT calculations in the same small basis 6-31G(d) with the dispersion correction GD2. The results of IR and Raman spectra calculations are presented in Fig. 2 and 3.

In the tetramer the form of normal vibrations remains the same like in molecular counterparts and occurs in each molecule one by one in turn. Small deviations of the structural molecular parameters in tetramer from those in single molecule immediately leads to the eight-fold splitting of the former generate modes and to the four-fold splitting of the former non-degenerate vibrations.

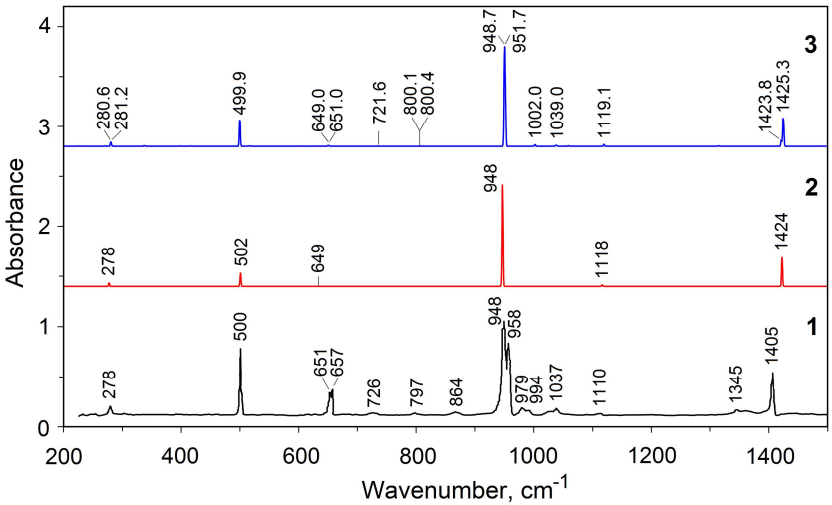

Fig. 2. Experimental IR spectrum of a red sample of compound **8S** (curve 1) [3] in comparison with that calculated for the free molecule **8S** (curve 2) and tetramer (curve 3).

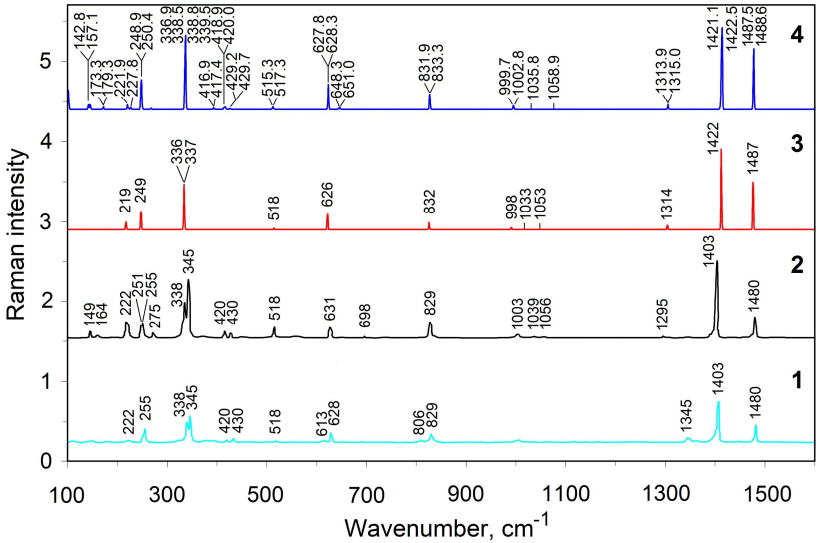

Fig. 3. Experimental Raman spectra of the white (curve 1) and red (curve 2) modifications sample of compound **8S** [3] in comparison with that calculated for the free molecule (curve 3) and tetramer (curve 4).

In the absence of symmetry all vibrations are allowed in the IR and Raman spectra and some normal vibrations provide additional weak bands in the observed experimental and calculated spectra. In the low-frequency range (less than 200 $см^{-1}$) we observe interesting phenomena: in the separate molecules of tetramer one can see mixing of different vibration types.

Below 80 $см^{-1}$ in the tetramer vibrational spectra we have calculated modes of translation and libration types. Among them in the Raman spectrum there are lines 44 and 77 $см^{-1}$ with the high calculated activity of 35 and

11 Å^4/amu, respectively. The first line is assigned to libration's mode and the second – to translational type of intermolecular vibration.

Thus, the tetramer simulation of crystal packing reproduces many fine-structure details in the octathia[8]circulene red species and affords assignment of vibrational IR and Raman spectra.

References

1. K. Yu. Chernichenko, V. V. Sumerin, R. V. Shpanchenko, E. S. Balenkova, and V. G. Nenajdenko, *Angew. Chem. Int. Ed.*, 2006, **45**, 7367.
2. J. H. Dopper, F. H. Wynberg, *J. Org. Chem.*, 1975, **40** (13), 1957.
3. S. S. Bukalov, L. A. Leites, K. A. Lyssenko, R. R. Aysin, A. A. Korlyukov, J. V. Zubavichus, K. Yu. Chernichenko, E. S. Balenkova, V. G. Nenajdenko and M. Yu. Antipin, *J. Phys. Chem. A*., 2008, **112**, 10949.
4. A. D. Becke, *J. Chem. Phys.*, 1993, **98**, 5648.
5. C. Lee, W. Yang, R. G. Parr., *Phys. Rev.*, 1988, **37**, 785.
6. M. M. Francl, W. J. Petro, W. J. Hehre, J. S. Binkley, M. S. Gordon, D. J. Defrees, J. A. Pople, *J. Chem. Phys.*, 1982, **77**, 3654.
7. A. D. Becke, *J. Chem. Phys.*, 2014, **140**, 18A301.
8. N. Mardirossian, M. Head-Gordon, *Mol. Phys.*, 2017, **115**, 1.
9. M. J. Frisch, G. W. Trucks, H. B. Schlegel, at al, Gaussian 16, Revision A.03, Gaussian, Inc., Wallingford CT, 2016.
10. P. L. Polavarapu, *J. Phys. Chem*., 1990, **94**, 8106.
11. S. I. Gorelsky, SWizard program, <http://www.sg-chem.net>, University of Ottawa, Ottawa, Canada, 2013.

LUMINESCENT SiO_2 NANOPARTICLES FOR CELL LABELING: COMBINED WATER DISPERSION POLYMERIZATION AND 3D CONDENSATION CONTROLLED BY OLIGOPEROXIDE SURFACTANT-INITIATOR

Nataliya Mitina[1], Catherine Cropper[2], Olga Klyuchivska[3], Khrystyna Harhay[1], Rostyslav Stoika[3], Orest Hevus[1], Yaroslav Z. Khimyak[2,4], Alexander Zaichenko[1]

[1]Department of Organic Chemistry, Lviv Polytechnic National University, Lviv, 79013, Ukraine
[2]Department of Chemistry, University of Liverpool, Liverpool, 7ZD, United Kingdom
[3]Department of Regulation of Cell Proliferation and Apoptosis, Institute of Cell Biology of NAS of Ukraine, Lviv, 79005, Ukraine
[4]School of Pharmacy, University of East Anglia, Norwich, 7TJ, United Kingdom,
e-mail: nmitina10@gmail.com

Hybrid polymer coated silica nanoparticles (NPs) were synthesized via low temperature graft (co)polymerization of trimethoxysilane propyl methacrylate (MPTS) initiated by surface-active oligoperoxide metal complex (OMC) in aqueous media and characterized using kinetic, solid-state NMR, TEM and FTIR techniques. Two processes, namely the radical graft-copolymerization due to presence of double bonds and 3D polycondensation provided by the intra- or/and intermolecular interaction of organosilicic fragments, occurred simultaneously. The relative contribution of the reactions depending on initiator concentration and pH value leading to the formation of low cured polydisperse

micro particles or OMC coated SiO_2 NPs of controlled curing degree was studied. The availability of free-radical forming peroxide fragments on the surface of SiO_2 NPs provides an opportunity for seeded polymerization leading to the formation of the functional polymer coated NPs with controlled particle structure, size, and functionality. Encapsulation of the luminescent dye (Rhodamine 6G) in SiO_2 core of functionalized NPs provided a noticeable increase in their resistance to photo-bleaching and good biocompatibility. These luminescent NPs were not only tolerated by the mammalian cells but also well attached to murine leukemia L1210 cells. This indicates their potential use for labeling of the mammalian cells.

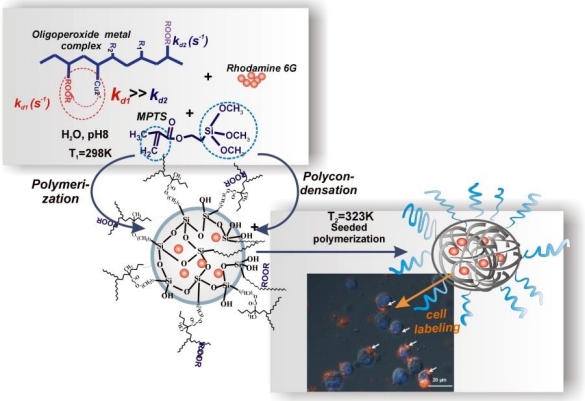

Fig. 1. A core-shell particle formation scheme as a result of water-dispersion polymerization of MPTS initiated by OMK, and murine lymphocytic leukemia L1210 cells treated for 24 h with Rhodamine G-conjugated NPs (micrographs of L1210 cells were taken using fluorescent microscopy after staining of cell nucleus material with Hoechst 33342 dye (blue fluorescence), while the NPs were stained in orange-red and seen attached to cell surface (white arrows)).

LEARNING ABOUT DNA BY MEANS OF CIRCULAR DICHROISM

Patrick Norman

Department of Theoretical Chemistry and Biology,
KTH Royal Institute of Technology,
SE-10609 Stockholm,
e-mail: panor@kth.se

There are two fundamentallydifferent ways to study DNA by means of circular dichroism spectroscopy: (i) a direct focus on the DNA fingerprint bands in the wavelength region of 250–300 nm that do not overlap with protein bands and which can reveal conformational changes, and (ii) an indirect focus on bands in the long wavelength region (λ> 300 nm) that do not overlap with DNA bands and which are associated with $\pi\pi^*$-transitions of biomolecular probes and for which the chirality is induced by the tertiary structure of DNA. We will discuss computational methodologies and some results for both these cases.

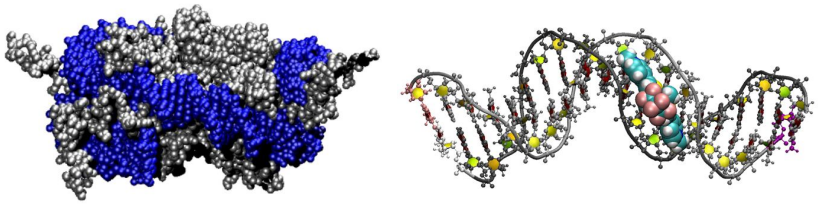

Fig. 1. Nucleosome core particle (left panel) with N-DNA (in blue) coiled around protein core histones(in grey) and biomolecular switch bound in the minor groove of a B-DNA sequence (right panel).

References

1. F. Di Meo, M. P. Pedersen, J. Rubio-Magnieto, M. Surin, M. Linares, P. Norman, DNA Electronic Circular Dichroism on the Inter-Base Pair Scale: An Experimental–Theoretical Case Study of the AT Homo-Oligonucleotide. *J. Phys. Chem. Lett.*, 2015, **6**, 355.
2. J. Rubio-Magnieto, F. Di Meo, M. Lo, C. Delcourt, S. Clément, P. Norman, S. Richeter, M. Linares, M. Surin, Binding modes of a core-extended metalloporphyrin to human telomeric DNA G-quadruplexes. *Org. Biomol. Chem.*, 2015, **13**, 2453.
3. N. Holmgaard List, J. Knoops, J. Rubio-Magnieto, J. Idé, D. Beljonne, P. Norman, M. Surin, M. Linares, Origin of DNA-Induced Circular Dichroism in a Minor-Groove Binder. *J. Am. Chem. Soc.*, 2017, **139**, 14947.
4. P. Norman, J. Parello, P. L. Polavarapu, M. Linares, Predicting near-UV electronic circular dichroism in nucleosomal DNA by means of DFT response theory. *Phys. Chem. Chem. Phys.*, 2015, **17**, 21866.
5. M. Linares, H. Sun, M. Biler, J. Andréasson, P. Norman, Elucidating DNA binding of dithienylethenes from molecular dynamics and dichroism spectra, submitted.

SORPTION OF CADMIUM IONS (II) ON THE SURFACE OF ORGANIC-SILICA MATERIALS MODIFIED BY PHOSPHONIC GROUPS

O. A. Orlova, I. V. Khristenko

Materials Chemistry Department,
V. N. Karazin Kharkiv National University, 61022, Kharkiv, Ukraine,
e-mail: khristenko@karazin.ua

The problem of analyzing the water resources and water treatment to ensure the necessary quality of drinking water is relevant for many countries, including Ukraine. The main pollutants of natural and waste water include heavy metals and their compounds. Common and yet inexpensive methods of analysis and purification of water from metal-containing compounds include sorption methods that ensure the most complete extraction of metal ions (especially from solutions with low concentrations). Various materials of natural and artificial origin are used as sorbents.

In contest of above mentioned problem the researchers are interested in hybrid organic-silica materials modified with phosphonic groups, which due to the presence of $-PO(OH)_2$ groups in their structure have a high sorption ability with respect to heavy metal ions.

The sorption of cadmium ions on the surface of a number of sorbents (silicagel with groups of aminodiphosphonic acid monopotassium salt, organic-silica material modified with diethyl 2-(3-

(triethoxysilane) propyl)amino-2,2-dimethylphosphonate) was investigated. The sorption of cadmium (II) ions on the surface of modified sorbents was studied by the method of individual samples. A sample of the sorbent was contacted with a solution of cadmium chloride with the concentration range from 1 to 0.007 mmol / g. The residual concentration of metal ions in the solution around the sorbent was determined by spectrophotometric and potentiometric methods.

For all the materials under consideration, a polymolecular adsorption isotherm was observed (Fig. 1), which indicates the formation of several types of complexes on the surface.

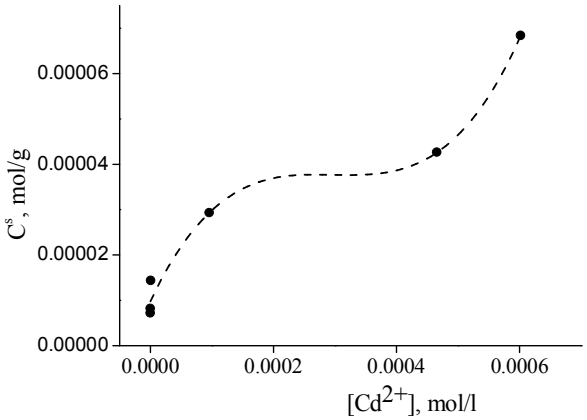

Fig. 1. Isoterm of sorption of Cd (II) ions at the surface of an organic-silica material modified by diethyl 2-(3-(triethoxysilane) propyl) amino-2,2-dimethylphosphonate).

The Fig. 2. shows the concentration of sorption of Cd (II) ions on the surface of the materials (mass of the sample 0.07 g) from a solution with an initial concentration of $CdCl_2$ 0.001 mol/l. The maximum adsorption of cadmium ions is observed for organic-silica material modified with diethyl 2-(3-(triethoxysilane) propyl) amino-2,2-dimethylphosphonate, which was obtained by sol-gel synthesis in the presence of ammonia.

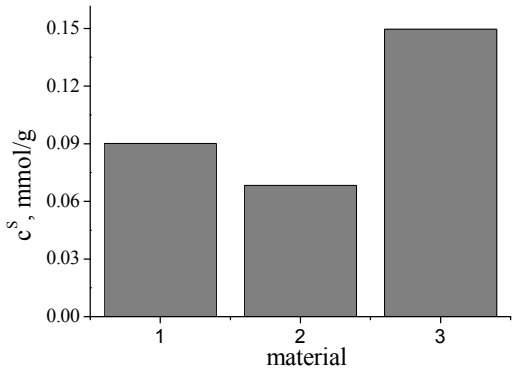

Fig. 2. The ratio of the concentration of sorption of Cd (II) ions on the surface of the materials.

LOW-TEMPERATURE THERMOLUMINESCENCE OF NANOCOMPOSITES OF SILICON ORGANIC POLYMER

Nina Ostapenko

Institute of Physics of NASU, *Prosp. Nauky 46, Kyiv 03028, Ukraine*
e-mail: nina.ostapenko@gmail.com

Abstract. Low-temperature termoluminescence (TSL) of poly(di-*n*-hexylsilane) (PDHS)/MCM-41 and PDHS/SBA-15 nanocomposites and solutions of PDHS polymer in tetrahydrofuran (THF) with different concentrations from 10^{-3} to 10^{-5} mol/l in the temperature range of 5–120 K was studied. It is shown that the maxima of the TSL curves of nanosized polymers and their FWHMs depend significantly on the pore diameter of nanoporous silicas. With a decrease in the pore diameter from 10 to 2.8 nm, the maximum of the TSL curve of the PDHS/MCM-41 nanocomposite is shifted by 33 K toward low temperatures, and its FWHM decreases by 50 K relative to the TSL curve of the polymer film. This effect is associated with the decrease in the number of polymer chains, and, accordingly, the number of traps on which charge carriers (CC) are localized in the nanosized polymer. In the PDHS/MCM-41 nanocomposite (2.8 nm), a minimum number of traps with a smaller energy distribution is observed compared with the polymer film. Thise changes in the TSL curves of nanocomposites are similar to those observed with the change in the concentration of polymer solutions. Investigation of TSL of nanocomposites based on

PDHS polymer introduced into nanoporous silicas with different pore diameters has shown the possibility of changing the number of CC traps and their energy distribution.

Introduction. The use of nanosized polymers in optoelectronics, microelectronics, and medicine gives reason to study their optical and electrical characteristics in order to produce materials with improved properties. Investigation of the PL of silicon organic polymers introduced into silica nanopores of different diameters has shown that it is possible to controllably select a certain number of polymer chains by changing the nanopore diameter. To study the processes of localization and release of CC from traps in PDHS nanocomposites, TSL is used. The intensity of the TSL and the shape of its curves are used to obtain information on the processes of capture, release, recombination of CC, and the properties of CC traps. This paper presents the results of TSL of PDHS polymer films, its PDHS/MCM-41 and PDHS/SBA-15 nanocomposites obtained by introducing the polymer into nanopores of MCM-41 and SBA-15 silicas with pore sizes of 2.8 and 10 nm, and solutions of PDHS in THF with different polymer concentrations in the temperature range of 5–120 K.

TSL investigation of PDHS polymer nanocomposites and polymer solution. Fig. 1 shows the TSL curves of the PDHS film, the nanosized PDHS polymer introduced into the nanopores of SBA-15 silica with a pore

diameter of 10 nm, and of the 10^{-4} mol/l solution of PDHS in THF. The TSL curve of SBA-15 silica has a maximum at 13 K. From Fig. 1 (curve 2) it can be seen that the TSL curve of the nanosized PDHS in the pore of SBA-15 has a broad band with a maximum at 25 K and a weak shoulder at 36 K. The maximum of the TSL curve of the nanosized PDHS polymer is shifted by 24 K relative to the maximum of the TSL curve of the polymer film towards low temperatures, and its FWHM is decreased by 18 K relative to the TSL curve of the film. It is known that the TSL curve of a polymer is related to the number of CC localized in traps, from which they are released when the temperature of the film increases. There are 6–7 polymer chains in SBA-15 pore (10 nm). In this case, the number of polymer chains and CC traps in the nanocomposite is smaller than in the polymer film. This relates to the shift of the maximum of the TSL curve of the nanosized PDHS towards low temperatures relative to the TSL curve of the film. The maxima of the TSL curves of the nanosized PDHS (curve 2) and the dilute solution of PDHS with concentration 10^{-4} mol/l are very close (curve 3). This indicates that the number of CC traps in these systems is almost the same.

The TSL curve of the PDHS/MCM-41 nanocomposite consists of a rather intense and narrow band with a maximum at 17 K, shifted relative to the maximum of the TSL curve of PDHS/SBA-15 nanocomposite in the direction of low temperatures by 8 K, and a weak shoulder at 28 K.

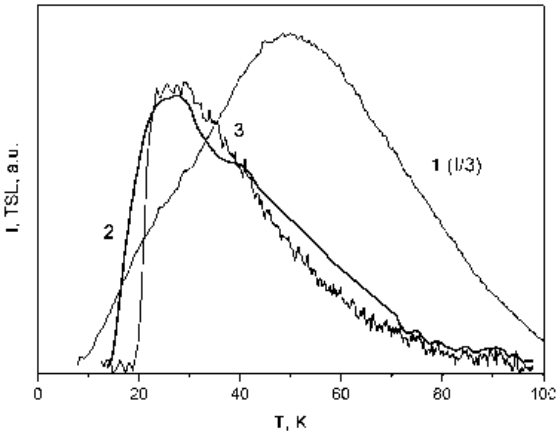

Fig. 1. TSL curves of the PDHS film (1), the nanocomposites PDHS/ SBA-15 (2), the solution of PDHS polymer in tetrahydrofuran at a concentration of 10^{-4} mol/l (3).

Since there is practically only one polymer chain in the MCM-41 pores, the number of CC traps in this case is less than for the PDHS/SBA-15 nanocomposite. This is associated with a shift in the maximum of the TSL curve of PDHS/MCM-41 nanocomposite toward low temperatures and the narrowing of its FWHM by 32 K with respect to the FWHM of the TSL curve of the PDHS/MCM-41 nanocomposite. The closeness of the maxima of the TSL curves of the PDHS/MCM-41 nanocomposite and the dilute solution of PDHS at a concentration of 10^{-5} mol/l indicates that these pores contain single polymer chains, a minimum number of CC traps and their energy distribution.

ELECTROLUMINESCENT PROPERTIES OF HETEROSTRUCTURES BASED ON CdTe/CdS QUANTUM DOTS

A. Pidluzhna[a], Kh. Ivaniuk[a], M. Chapran[b], O. Tynkevych[c], Yu. Khalavka[c] and P. Stakhira[a]

[a] Lviv Polytechnik National University,
St.Bandery st. 12, Lviv 79013 Ukraine
e-mail: Anna.Y.Pidluzhna@lpnu.ua
[b] Lodz University of Technology,
Zeromskiego 116, 90-924 Lodz, Poland
[c] Yuriy Fedkovych Chernivtsi National University,
L. Ukrainky st. 25, Chernivtsi 58012 Ukraine

The search of different technics for synthesis, investigation of physical and chemical properties and areas of application for quantum dots QD has being attracted a great interest over a few decades [1–3]. Such materials as CdSe, CdTe, CdS are the subject of special scientific interest thanks to the change in properties of semiconductors with transfer to nanoscale of particles size [3, 4].

Extensive list of works is attributed to semiconductive nanoparticles application in light emitting diodes LED field. The new trend of LED technology is a QD application in manufacturing of complex optical structures for enrichment of basic pallet and optically active materials [4]. The nanocrystal-based light emitting diodes demonstrate sizeable increase in the external quantum efficiency and improve color emission pallet [5].

This work deals with application of water solution of CdTe/CdS nanoparticles in organic LED. The structure ITO/MoO_3/QD/TPBi/Al was successfully formed and its optical parameters were determined (Fig. 1).

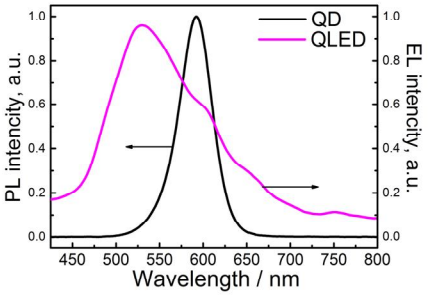

Fig. 1. Photoluminescence intensity of CdTe/CdS nanoparticles in water media (black) and Electroluminescence intensity of ITO/MoO3/QD/TPBi/Al structure with CdTe/CdS quantum dots (magenta).

References

1. D. Chirvase, J. Parisi, J. C. Hummelen, V. Dyakonov, *Nanotechnology*, 2004, **15**, 1317.
2. V. Dyakonov, J.L. Delgado, *Advanced Energy Materials*, 2017, **7**, 1700252.
3. R. Khairutdinov, *Uspechi Chimii*, 1998, **67**, 125–139.
4. Chun Hao Lin, Evan Lafalce, Jaehan Jung et al., *ACS Photonics* 2016, **3**, 647–658.
5. Xing Xia, Zuli Liun, Guihuan Du et al., *Journal of Luminescence*, 2012, **132**, 100–105.

INDIRECT SPECTROPHOTOMETRIC DETERMINATION OF REDUCTION AGENTS WITH *N,N,N′,N′*-TETRAETHYLBENZIDINE

Oleg Pogrebnyak, Sergey Bondarchuk, Nelia Ridchenko and Julia Tishena

Bohdan Khmelnytsky Cherkasy National University, Cherkasy, Ukraine
e-mail: pogrebniak-oleg@ukr.net

The current problems of the environment require analysts to develop new methods and analysis techniques that are characterized by a high sensitivity, accuracy and speed. Among the harmful substances that pollute natural landscapes we can highlight sulfides, thiocyanates, hydrazine and its derivatives. These toxicants have both the natural and industrial sources of environmental influx.

To date, a number of methods have been proposed to determine these substances. With a good selection of reagents and determination conditions, however, the spectrophotometric method prevails on the classical chemical methods in many metrological characteristics. Moreover, compared with many instrumental methods, the spectrophotometric method has low cost and availability along with satisfactory sensitivity. Therefore, the development of new indicator systems for spectrophotometric determination of toxicants in the environmental objects and foods remains an urgent task of contemporary analytical chemistry.

It has been shown earlier [1, 2] that *N,N,N′,N′*-tetraethylbenzidine (TEB) in an acidic medium is oxidized with hypochlorite to form *N,N*-diethylaminodichinone cation. Such chemistry of the process is confirmed by the corresponding quantum-chemical calculations [3]. The light absorption of the reaction product at 475 nm varies directly proportional to the concentration of hypochlorite; this is the basis of its spectrophotometric, colorimetric and test determination [4]. The aim of the present work was to study the possibility of use of the above-mentioned indicator system for indirect spectrophotometric determination of reducing agents, in particular, sulfides, thiocyanates and hydrazine.

As a result, a new spectrophotometric indirect method for sulfide, thiocyanate and hydrazine determination was proposed. The method is based on the oxidation of an appropriate reagent by a known excess of hypochlorite followed by a measurement of absorbance of the product of TEB oxidation with the remaining hypochlorite at 475 nm. When determining optimum conditions of the reaction and verification of its suitability for analytical purposes, we have investigated the relationship between TEB oxidation products and the molar ratio $n(ClO^-)/n(red)$ in the initial solution of the reagent, the exposure time of the reaction mixture, the optimum reagent concentrations and acidity of the medium.

The detection limits (by 3*s* criterion) for sulfide, thiocyanate and hydrazine are 0.10, 0.12 and 0.07 mg·L^{-1}, respectively. Their calibration curves are linear in the concentration ranges 0.1–0.7, 0.4–4.0 and 0.1–1.4 mg·L^{-1}, respectively ($s_r \leq 0.04$, $n = 5$).

The metrological characteristics of the procedure were checked using the working samples. Results of the testing methods satisfactory prove its accuracy and convergence. The effect of foreign ions in determination of the corresponding ions was studied. It has been established that most of the components, such as natural water, do not interfere with the ions under determination. The reagents are accessible and resistant over time. Additionally, the proposed procedure is simple and suitable for specified ions determination in various objects.

References

1. O. A. Zaporozhets, O. S. Pogrebnyak, N. N. Vizir, *J. Water Chemistry and Technology*, 2011, **33**(1), 31.
2. O. A. Zaporozhets, O. S. Pogrebnyak, N. N. Vizir, *J. Anal. Chem,* 2012, **67**(8), 694.
3. Б. П. Мінаєв, Н. Є. Карловська, О. В. Білий, *Вісн. Черк. Унів. Серія Хім. Науки*, 2012, **227**(14), 29.
4. О. С. Погребняк, *Вісн. Черк. Унів. Серія Хім. Науки*, 2013, **267**(14), 96.

LABEL-FREE CONFOCAL IMAGEING OF LIVING CELL. HYPOTHESIS AND SUPPOSITIONS

Ivan Polovyi [1], Olena Gnatyuk [1], Denys Bilko [2], Nadiia Bilko [2], Marharyta Pakharenko [2], Sergii Karakhim [3], Galina Dovbeshko [1]

[1]Department of Physics of Biological Systems, Institute of Physics, NAS of Ukraine, 46, prospect Nauky, 03680, Kyiv, Ukraine

[2]Department of Natural Science, The National University of Kyiv-Mohyla Academy, 2, Skovorody St., Kyiv, 04655, Ukraine

[3]Department of Muscular Biochemistry, Palladin Institute of Biochemistry, NAS of Ukraine, 9, Leontovycha St., 01601, Kyiv, Ukraine

e-mail: ipoliovy@gmail.com

It is well-known that weak fluorescence appears in some types of living cells under biological proceses such as metabolite activity, oxidation, proton transfer, aging etc [1]. There are data [2] that suggest fluorescent enhancement effect to be connected with metal nanostructured substrate. Earlier we have registered weak emission from unstained living cells under confocal microscopy. The reason of it is not clear. So, the questions arise – what cellar component and cell process is responsible for it.

Here we want to summarize our experimental data and give possible direction to look for explanation of observed phenomenon.

In [3] was shown that rough nanostructural gold surface used as substrate enhances a fluorescence of biological objects, including living cells. We studied self-luminescence of living and apoptotic cell on rough nanostructural gold and glass substrateand observed green and blue fluorescence.

Two types of cell lines were cultivated on gold and glass substrate – MCF-7 (human breast cancer line) unstained cells and HS-5 (human bone barrow stromal fibroblast) modified with GFP (green fluorescent protein). Apoptosis was initiated either with cold shock or hydrogen peroxide and confocal images were obtained with LSCM (Carl Zeiss, Germany) with excitation emission of 633 nm 543 nm 488 nm 405 nm.

As we observed, apoptotic cells of both lines possessed less intense luminescence in green and blue regionand more intense in red region compared to living cells. Moreover, this emission was enhanced with gold substrate. In our previous study [3] SPEV cells on gold substrate showed pronounced fluorescence unlike fibroblast cells, which appeared dark spots in contrast to bright gold background. We suppose that the highly active cells are those which give noticeable emission. They are cancer cells, stem cells, apoptotic cells. We believe that mitochondria and nucleus are the key elements of luminescence effect since they hold numerous cell processes and bimolecular transformations.

The biological reason of emission could be connected with biological effect – disruption of crowding or molecular condensation. Physical reason of it seems in light scattering on spherical and cylindrical objects of nanometer size which may serve as light nanolens and nano-jets [4] as well parametric scattering effects or parametric luminescence [5]. Both biological and physical effects is subject for future study.

References

1 J. M. Levitt, A. Baldwin, A. Papadakis, *et al.*, *J. Biomed. Opt*. 2006, **11**, 064012.

2 J. R. Lakowicz, J. Malicka, I. Gryczynski, *Biotechnique,* 2003, **34**, 62–68.

3 G. I. Dovbeshko, O. P. Gnatyuk, S. O. Karakhim, *Semicond Ph, Quan Electron & Optoelectronics*, 2017, **20**, 159–167.

4 B. S. Luk'yanchuk, R. Paniagua-Domínguez, I. Minin, O. Minin, Z. Wang, *Optical Materials Express*, 2017, **7**, 1820–1847.

5 G. X. Kitaeva, A. N. Penin, *J. Exp. Theor. Phys.,* 2005*,* ***82***, 388–394.

WASTE-FREE RECYCLING OF SLUDGE WASTES OF "CHERKASY KHIMVOLOKNO"

Yulia Shaforost, Rostislav Galagan, Yaroslav Korol, Tetyana Zaporozhets and Vira Boyko

Department of Chemistry and Nanomaterials Science, Bohdan Khmelnitsky National University, 18031, Cherkasy, Ukraine,
e-mail: ZdorYulia@ukr.net

In this paper, a laboratory study of the properties of zinc-containing sludge obtained after the recycling of waste from the viscose fiber production, has been carried out by the calcium hydroxide method. A waste-free process of complex recycling of such sludge was developed.

On the basis of this method, the design and construction of a semi-industrial sludge processing unit located in the sludge storage facilities of "Cherkasy Khimvolokno" can be carried out. A scheme of complex processing of zinc sludge produced by "Cherkassy Khimvolokno" is offered. For sufficiently complete removal of organic compounds, the initial sludge was calcined in a muffle furnace at 900 °C for 1 hour. The sludge, after calcination, was investigated on an X-ray fluorescence spectroscopy on the content of metallic elements. The corresponding spectrum is shown in Fig. 1.

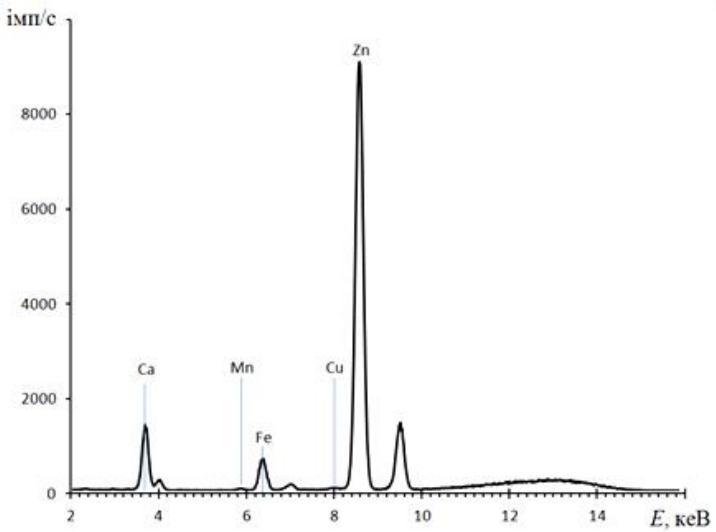

Fig. 1. Spectrum of initial sludge after calcining.

The recycling scheme is based on the treatment of roasted sludge with concentrated nitric acid. With this treatment, all soluble calcium, as well as iron and zinc, are transferred to the solution. Residual precipitate, which is insoluble in nitric acid and consists mainly of calcium sulfate, is filtered off. The formed filtrate was alkalized to pH 4.2 to separate iron from zinc in the form of $Fe(OH)_3$. After separating Zinc in the filtrate remain soluble calcium nitrate and sodium nitrate. Calcium nitrate in the interaction with calcium soda gives calcium carbonate (Fig. 2).

Control of products at each stage of the process was carried out by X-ray fluorescence spectroscopy, X-ray diffraction and chemical methods.

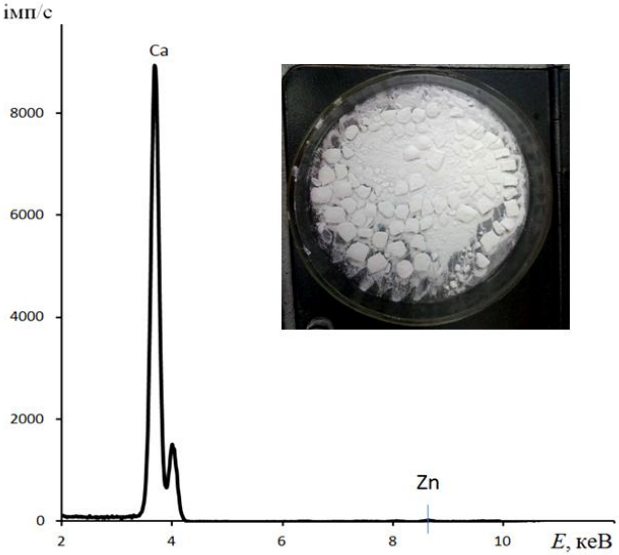

Fig. 2. Spectrum $CaCO_3$

Conditions of each stage in the laboratory process are specified. Impossibility of the waste-free sludge processing without roasting of its organic constituents is proved. It is shown that the final products of such processing can be: the powder for salt-affected soils reclamation, gypsum, ferric oxide, zinc oxide, metallic zinc, chemically precipitated chalk, sodium nitrate.

References

1. Сорокіна К. Б., Козловська С. Б. Технологія переробки та утилізації осадів: Навч. Посібник. – Харк. нац. акад. міськ. госп. – Харків: ХНАМГ, 2012. – 226 с.
2. В. И. Таллин, В. И. Шматова, *Химические волокна*, 1984, **4**, 48–50.

3. Г. М. Атамась, Г. С. Столяренко, *Вопросы химии и химической технологии*, 2008, **3**, С. 76–79.
4. Патент 2138570 Россия, МПК C22B19/00 Способ гидрометаллургического получения оксида цинка / И. И. Нечаев, В. А. Артющик. № 9910011/02: Заявл. 10.01.1999: Опубл. 27.09.1999, Бюл. № 27. 7с.
5. Патент 10800 України, МПК C22C1/16 Спосіб видобування цинку / Б. І. Байрачний, Л. В. Трубнікова, В. М. Скорикова, Л. О. Гудевич, Л. В. Козорезова, Л. М. Дмітрієва № 930094; Заявл. 16.12.1993; Опубл. 25.12.1996, Бюл. № 4. 5 с.
6. M. K. Jha, V. Kumar, R. J. Singh, *Resources Conservation and Recycling*, 2001, **33**, (1) 1–22.
7. M. K. Jha, V. Kumar, L. Maharaj, R. J. Singh, *Ind. Eng. Chem. Res.*, 2004, **43**, 1284–1295.

EMISSION OF SPECTRAL BANDS AND LINES AT ELECTRON IMPACT EXCITATION OF GAS-PHASE GUANINE MOLECULES

I. I. Shafranyosh, Yu. Yu. Svida, M. I. Sukhoviya and M. I. Shafranyosh

Uzhgorod National University, 88000 Uzhgorod, Ukraine
e-mail: ivanshafr@gmail.com

In the present work, we carried out the experiments by the optical method, which had been used before [1]. The gas phase of guanine molecules was formed through the heating of the guanine polycrystalline powder in a separate stainless steel container. The electron beam was formed by the three-electrode gun with a tungsten cathode.

As a result of research, the luminescence spectra of guanine molecules in gas phase are obtained in the wavelength range of 200–500 nm under the influence of electron beams of different energies. The results of experimental measurements for electron energies of 20, 40, 60, 80 and 100 eV are shown on Fig. 1, where the luminescence intensity is set on y-axis in absolute units, and the wavelengths in nanometers (nm) are set on x-axis. The spectral sensitivity of the spectrophotometer is taken into account in the given spectrum. As can be seen from Fig. 1, twentymolecular bands and lines are shown in the spectra of guanine in gas phase. Their maxima are located at the following wavelengths: $\lambda_m\lambda_m$ = 289.2; 304.2; 307.2; 315.9; 326.5; 337; 355.3; 357.7; 362; 367.1; 386.1; 388.2;

391.6; 395.4; 412.4; 415.5; 430.5; 434.4; 447.3; 486.1 nm. The quantity and shape of the spectral bands indicate that the nature of their origin is connected with the excitation of the electronic states of both the whole molecule and its ionized or neutral fragments (dissociative excitation, dissociative excitation with ionization). Practically all bands have a complex character and it testifies to their superposition nature.

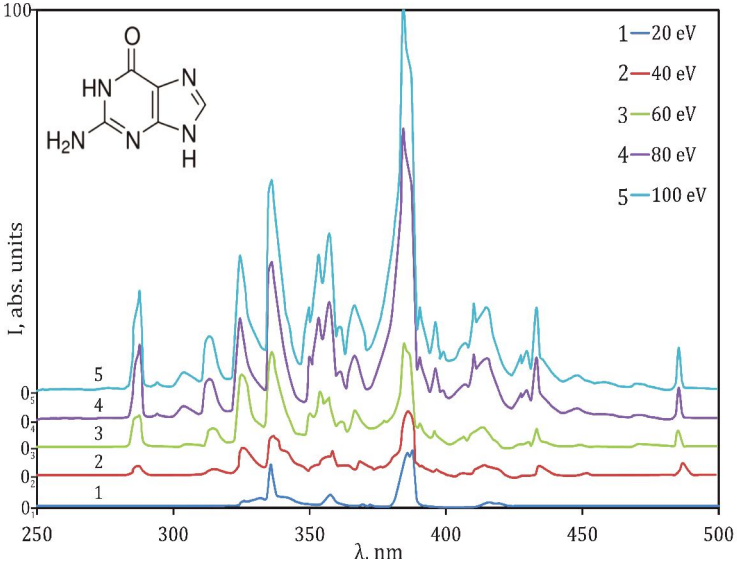

Fig. 1. Luminescence spectra of the guanine molecules for different electron energies.

It is rather difficult to identify the spectral bands because of the extremely scarce data available in the literature. However, despite it, we succeeded to perform the following analysis of the nature and origin of the bands in the luminescence spectrum of guanine. For this purpose, the photoemission spectra of polyatomic chemical

compounds [3–5] were taken into account; the results of the mass-spectrometric research of guanine and adenine molecules were used; the data concerning the effective cross-sections of complete and dissociative ionization of both purine bases by electron impact [2] were applied.

The spectral line at the wavelength λ = 486.1 nm belongs to the hydrogen atom (H_β line of the Balmer series) and, by the way, is observed in the spectra of other nitrogenous bases [1]. Therefore, the important physical conclusion comes that the significant quantity of hydrogen atoms is formed in biological structures under the influence of electrons. The bands at the wavelengths λ = 447.3; λ = 430.5 nm probably belong to the group CO ($B^1\Sigma^+ \rightarrow A^1\Pi$). The excited fragments CH ($A^2\Delta \rightarrow X\ ^2\Pi$), N_2 ($C^3\Pi_u \rightarrow B^3\Pi_g$), H_2CN_2 ($\tilde{A} \rightarrow \tilde{X}$) can take part in the formation of the band at λ = 434.4 nm. We are inclined to think about the preferred contribution of the fragment H_2CN_2in formation of the above band, the narrow line at λ = 434.1 nm belongs to Hγ line of the Balmer series. The wide band with the maximum at λ = 415.5 nm is formed by several groups: in particular, CO ($B^1\Sigma^+ \rightarrow A^1\Pi$), at the wavelength of λ = 412.4 nm and CO^+ ($B^2\Sigma^+ \rightarrow A^2\Pi$) at λ = 395.4 nm. The intensive band at λ = 388.2 nm is formed by the fragments CO ($C\ ^1\Sigma^+ \rightarrow A\ ^1\Pi$) and CN ($B\ ^2\Sigma \rightarrow A\ ^2\Pi$). Here the main contribution belongs to the group CO, because the excitation effective cross-section of the electronic transition ($C^1\Sigma^+ \rightarrow A^1\Pi$) in CO is significant. The intensive band at λ = 386.1 nm is formed by the fragments CN ($B\ ^2\Sigma \rightarrow A^2\Pi$) and CNC ($\Delta^2 \rightarrow\ ^2\Pi$). The contribution from

the CN radical can be considered to be predominant. Band at λ = 367.1 nm with insignificant intensity belongs to CO^+ ($B^2\Sigma^+ \rightarrow A^2\Pi$). The band at λ = 357.7 nm can be formed by the fragment HCN_2. The band at λ = 355.3 nm is probably formed by the fragments HNCN ($\tilde{A} \rightarrow \tilde{X}$) and N_2 ($C\ ^3\Pi_u \rightarrow B^3\Pi_g$), but the contribution of each of them to the formation of this band is not known yet. The band at λ = 337nm should be identified as the superposition of the transitions ($C\ ^3\Pi_u \rightarrow B^3\Pi_g$) molecule $N_2$and ($^3\Pi_u \rightarrow\ ^3\Sigma_g^-$)NCN fragment. The band at λ = 326.5 nm can be formed by fragments CN^+ and NCN ($\Delta^2 \rightarrow\ ^2\Pi$), however the contribution of each of them is not determined yet. Note that the radiation in the wavelength range from 367.1 nm to 395.4 nm is located on the very wide band, which serves as a peculiar lining for them. In our opinion, this wide band is the revealing of luminescence as a result of excitation of π-electrons in guanine molecules.

References

1. I. I. Shafranyosh, M. I. Sukhoviya, *J. Chem. Phys.*, 2012, **137,** 184303.
2. B. F. Minaev, M. I. Shafranyosh, Yu. Yu. Svida, M. I. Sukhoviya, I. I. Shafranyosh, G. V. Baryshnikov, V. A. Minaeva, *J. Chem. Phys.*, 2014, **140**, 175101.
3. K. P. Huber, G. Herzberg, *Molecular spectra and molecular structure*, 1979, **4**, 716.
4. G. Herzberg, *Molecular spectra and molecular structure*, 1966, **3**, 745.
5. R. W. Pearse, A. G. Gaydon, London: Chapman, 1963, 562.

ELECTROCHEMICAL REDUCTION OF SALICYLIC ACID ON THE NICKEL ELECTRODES MODIFIED BY CHROME

Oleksandr Shevchenko[1], Olena Lut[1], Olena Aksimentyeva[2]

[1]Department of Chemistry and Nanomaterials Science, Bohdan Khmelnytsky National University, 18031, Cherkasy, Ukraine,
e-mail: Lutlen@ukr.net
[2]Department of Physical and Colloid Chemistry, Ivan Franko National University of Lviv, Ukraine
e-mail: aksimen@ukr.net

Voltamperometry and chronopotentiometry are commonly used electrochemical methods for the investigation and analysis of organic compounds. The successes in this field of electroanalysis are associated with the emergence of a new generation of electrodes - chemically modified electrodes (CME). The chemical modification of the electrode surface gives it special properties that contribute to the sensitivity, selectivity and reproducibility of the method. The important biological, analytical and industrial value of salicylic acid (SA), widely used in medicine, the production of biological drugs, medicines, and food products is due to the considerable interest of researchers in the reactions of the transformation of the SA under the influence of various factors, in particular, accompanied by the transfer of electrons in oxidation-reduction processes. At the same

time, the toxic effect of significant concentrations of SA causes the need to find methods for its identification and disposal, both in the manufacture of medicinal products, and in the treatment of sewage. At present, the use of electrochemical research methods for the analytical determination of SA in complex reactions involving intermediates is important. However, in studing the electrochemical behavior of the SA, special attention is given to the study of oxidation-reducing processes on electrodes of various nature.

The purpose of the work is to study the process of salicylic acid reduction on the surface of nanostructured and smooth nickel electrodes modified with micro quantity of chromium.

With the use of cyclic voltammetry and chronopotentiometry, the process of electrochemical reduction of salicylic acid on the surface of nanostructured and smooth electrodes with electrodeposited chromium was studied. It was established that the reduction process on both electrodes proceeds at close values of the electrode potential, but on nanostructured electrode it is almost twice more intense. The nature of the first maximum, which corresponds to the potential - 0.45 - 0.5 V, is related to the discharge of the ions of hydroxonium. The process of reduction of the investigated depolarizer passes at potentials close to 1.0 V, which corresponds to the second maximum of current at the current-voltage curve and the bend on chronopotentiometric curves (Fig. 1, a, b).

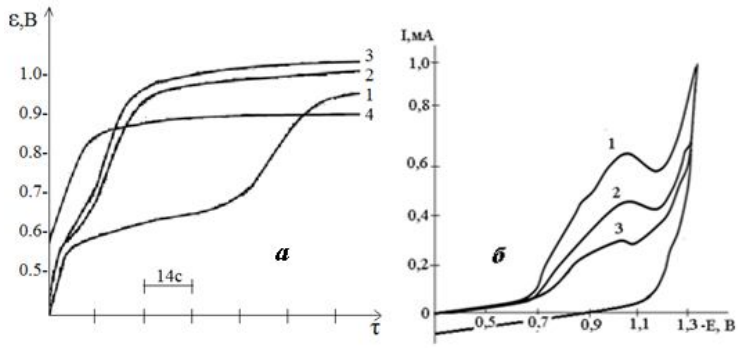

Fig. 1. (a) Chronopotentiometric curves at different concentration of SA: 1. $c = 9 \cdot 10^{-3}$ mol/dm^3; 2. $c = 6 \cdot 10^{-3}$ mol/dm^3; 3. $c = 5 \cdot 10^{-3}$ mol/dm^3; 4. Background curve $LiClO_4$ – 0,5 mol/dm^3; current density $6{,}3 \cdot 10^{-4}$ A/cm^2; **(b)** cyclic voltampere curves of reduction of SA at concentrations: 1– 0.0065 M; 2 – 0.005 M; 3– 0.004 M on the electrode with the acute structure of nickel and additionally deposited chromium: (pH = 0.88; T = 293 K; $\upsilon = 2 \cdot 10^{-2}$ V/s).

It was investigated that the recovery currents increase in proportion to the concentration of salicylic acid on a smooth and nanostructured electrode, which can be used for voltamperometric determination of SA in aqueous solutions. In our studies for solutions of salicylic acid at intervals of concentrations $3 \div 9 \cdot 10^{-3}$ mol/dm^3 and at current density $6{,}3 \cdot 10^{-4}$ A/cm^2 for nanostructured electrode, in terms of the apparent surface, the dependence $\tau^{1/2} - c_0$ for the chronopotentiometric curves has a linear character. This dependence allowed obtaine an equation

for quantitative definitions of SA: $\tau^{1/2} = K \cdot c_0$, where K according to our calculations was $0.56 \cdot 10^3$.

Calculated from voltammetric and chronopotentiometric curves, the diffusion coefficients and the rate constants of the electrochemical process on the surface of smooth and nanostructured electrodes are well correlated with each other, which indicates a similar mechanism of electroreduction. The calculated value of the heterogeneous rate constant is $k_s = 8.4 \cdot 10^{-6}$ m/s, which is characteristic for the irreversible process [1]. The dependences E_{max}- lg υ are linear, having the same angle of inclination, chronopotentiometric curves drawn on the scale of potentials (Fig. 1a) confirm the irreversibility of the process of reduction of the depolarizer on the electrodes under study.

References

1. O. Shevchenko, O. Lut, O. Aksimentyeva, *Visnyk of Cherk. Univ. Ser. Chem. Sci.*, 2013, **14** (267), 79–85.

THE ESTIMATION OF TETRABUTOXYTITANE CATALYTIC ACTIVITY IN THE SUBSTITUTED BENZOIC ACIDS ARYLIDES SYNTHESIS BY MEANS OF NMR^{1}H-SPECTROSCOPY METHOD

Leon Shteinberg

Department of Scientific Researches, Crop Care Institute, 18031, Cherkasy, Ukraine
e-mail: leon.shteinberg@ukravit.ua

Arylides of aromatic carboxylic acids widely used as basis of pesticidal compositions. Their synthesis by the direct catalytic amidation of carboxylic acids by amines is the intensively developed method within the framework of conception of «green chemistry» [1, 2].

It is before found [3, 4], that the effective catalyst of such compounds synthesis is tetrabutoxytitane (TBT) and products of his partial hydrolysis – polybutoxytitanates (PBT). It is set that last, in a number of cases, are substantially more effective, than TBT. Accordingly, all ecological parameters of such process (expense of heat on heating of reactionary mass and raw material constituents; amount of appearing liquid and hard wastes and technological stages) can be optimized by the selection of more active catalyst.

Unfortunately, technical standards on TBT and measureable on their basis indexes of quality do not give an answer for a question about his catalytic activity.

The hydrolysis of TBT is studied in more detail by means of different physical and chemical methods, and properties of hydrolysis products are confronted with their catalytic activity in the model reaction of benzoic acid with an aniline.

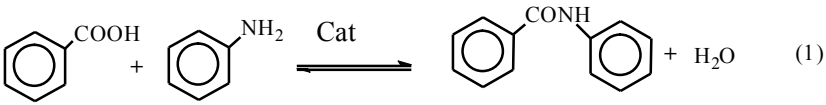

(1)

Cat. = TBT, PBT

The terms of preliminary even hydrolysis of TBT, dissolved in ortho-xylene or carbon tetrachloride, in a moist chamber are neat.

It is set that the method of NMR^{1}H spectroscopy allows well to trace cooperation of TBT with water, being in moist air. It was thus succeeded not only to identify the separate products of hydrolysis but also in number to count up molar correlation water :TBT (1,6 – 1,8) required for creation of effective catalyst.

The less of water activates TBT small, and greater – results in his complete deactivation, attended with the loss of catalytic activity and falling out from solution of hard hydrolysis products.

The new method of analysis allows to control activation of TBT by water and create catalysts on his basis, in ten of one times excelling last on the activity. It, in turn, substantially improves all ecological indexes of production process of aromatic carboxylic acidsarylides.

References

1. H. Lundberg, F. Tinnis, N. Selander, H. Adolfsson,*Chem. Soc. Rev*. 2014, **43**, 2714.
2. C. L. Allen, *Thesis doctor of philosophy*. University of Bath. 2012, 1-239.
3. L. Ya. Shteinberg, S. A. Kondratov, S. M. Shein, *Zhurn. Organ. Khimii.,* 1988, **24**(9), 1968.
4. L. Ya. Shteinberg, S. A. Kondratov, S. M. Shein, *Zhurn. Organ. Khimii.,* 1989, **25**(9), 1945.

A STRATEGY FOR CONVERTING INHERENTLY DIM PHOSPHORS INTO BRIGHT PURELY ORGANIC LONG-LIFETIME LUMINOPHORES

Asko Uri and Erki Enkvist

Institute of Chemistry, University of Tartu, 50411, Tartu, Estonia
e-mail: Asko.Uri@ut.ee

In course of development of inhibitors and photoluminescent probes for protein kinases we discovered [1, 2] organic tandem luminophores incorporating a covalently bound thiophene- or selenophene-comprising heteroaromatic fragment and a green, orange or red fluorescent dye whose absorption spectrum overlapped with the phosphorescence emission spectrum of the phosphor (Fig. 1). In water solution at room temperature the luminophores reveal intensive photoluminescence with slow decay (luminescence lifetime τ in the range of 20–300 μs) if they are specifically bound to the active site of a protein kinase (the latter molecule hinders molecular motions and shields the luminophore from the effect of dissolved molecular oxygen and other quenchers).

We suppose that the tandem luminophores possess efficient Förster-type resonant energy transfer (FRET) from the excited triplet state of the low-QY donor phosphor ($^3D^*$) to the adjacent acceptor fluorophore A ($^3D^* + {}^1A \rightarrow {}^1D + {}^1A^*$) [2] that leads to emission of light from the fluorescent dye. If the absorption spectrum of the acceptor fluorescent dye

has good overlap with the phosphorescence emission spectrum of the donor phosphor and the dye possesses high brightness, substantial (20–500-fold) enhancement of luminescence occurs [4]. Long lifetime of the emission mediated by the short-lifetime fluorescent dye is due to slow energy transfer (ET) from $^3D^*$ to the acceptor dye. As the emission is mediated by the fluorescent dye, the delayed photoluminescence spectrum of the tandem dye coincides with fluorescence emission spectrum of the attached dye. We have used probes comprising tandem luminophores for analysis of kinases in biological samples, screening of inhibitors in biochemical assays, and for mapping and monitoring activity of kinases in living cells using time-gated luminescence microscopy.

Now we have established that in solid PVA matrix, certain sulfur- or selenium-comprising heteroaromatic compounds possess remarkable phosphorescence with lifetime in millisecond region. Almost complete interchromophore ET from such donor phosphor, initially in excited triplet state, to an adjacent covalently linked acceptor fluorescent dye takes place if the donor and acceptor are covalently connected by a short linker. Variation of length of the linker enables tuning of luminescence lifetime in 100 μs to 5 ms range.

Excellent harvesting of energy of the triplet exited state of otherwise dim (possessing low quantum yield at room temperature) organic phosphors by adjacent fluorophores whose absorption spectrum overlaps with phosphorescence emission spectrum of the donor

phosphor, seems to be a general technology that may be applicable for construction of photoluminescence-based sensors for temperature and analytes (e.g., oxygen). The ET mechanism might also be applicable for development of efficient OLEDs, acting through harvesting of energy of electrically generated triplet excitons *via* emitting light by adjacent fluorescent dyes. Cheap chemicals and simple synthetic procedures would be used for construction of devices to compel the triplet excitons to emit light and to do useful work in OLEDs [3,4]. Heavier atoms than sulfur are not required to construct bright orange, red or near-infrared organic emitters possessing PL decay time in microsecond or millisecond range.

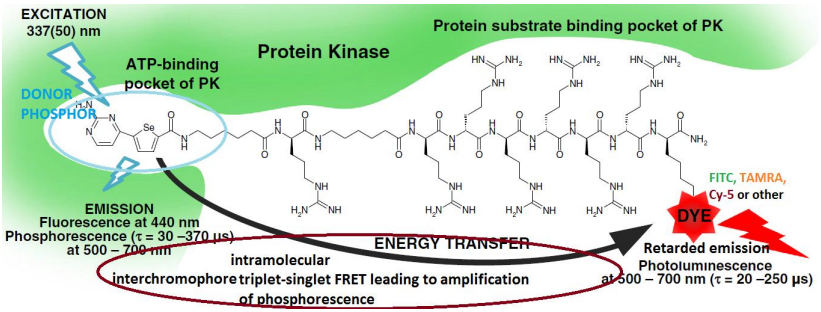

Fig. 1. Organic tandem luminophore-based probes for analysis of protein kinases.

The described phenomena follow the previous knowledge related to the occurrence of radiationless interchromophore triplet-singlet ET in different molecular systems. The feasibility of occurrence of ET from a donor in excited triplet state to an acceptor dye due to dipole-dipole

interactions was first theoretically suggested by Theodor Förster in 1959 [5]. Soon after that the phenomenon was demonstrated experimentally at cryogenic temperatures in a number of publications (first reported by ERMOLAEV and SVESHNIKOVA in 1962 [6]). Several review papers dedicated to the explanation of the ET mechanism. [5]

Additionally, in a series of papers [7], Lakovicz et al. analyzed the photoluminescence of tandem luminophores comprising covalent conjugates of transition metal-ligand complexes (possessing slow luminescence decay) and fluorescent dyes. They demonstrated that with reasoned combination of interacting chromophores and their positioning it is possible to construct tandem luminophore whose luminescence is substantially stronger than that of the distinct long life-time low quantum yield donor.

Work was supported by Grant IUT20-17 from ETAG.

References

1. E. Enkvist et al., *ACS Chem Biol.*, 2011, **6**, 1052.
2. K. Ligi et al., *J Phys Chem B*, 2016, **120**, 4945.
3. T. Förster, *Discuss Faraday Soc.*, 1959, **27**, 7.
4. B Minaev et al., *Phys. Chem. Chem. Phys.*, 2014, **16**, 1719.
5. D. Volyniuk et al., *J. Phys. Chem. C*, 2013, **117**, 22538.
6. Ermolaev V. L. and Sveshnikova E. B. Presentation at the 11th Conference on Luminescence (Minsk, September 1962): reported in УСПЕХИ ФИЗИЧЕСКИХ НАУК, Т. LXXX, вып. 4 (1963), С. 685.
7. B. P. Maliwal et al., *Anal. Chem.*, 2001, **73**, 4277.

MOLECULAR "LEGO-LIKE" ASSEMBLAGE OF FUNCTIONAL POLYAMPHIPHILS OF BLOCK/BRANCHED STRUCTURES

Alexander Zaichenko, Nataliya Mitina, Khrystyna Harhay, Olena Paiuk, Nataliya Kinash, Orest Hevus

Lviv Polytechnic National University, Institute of Chemistry, Department of Organic Chemistry, Lviv 79013, Ukraine
e-mail: zaichenk@polynet.lviv.ua

Developed synthesis and properties of functional polyamphiphils (PA) and self-assemblies (SA), micelles, interpolyelectrolyte complexes, nanoparticles (NPs), of desired size and functionality is discussed. Combined radical and non-radical methods of the synthesis of primary oligomer-precursors containing terminal or side reactive groups and their using for LEGO-like assemblage of PA of block and/or comb-like structures were studied. Proposed approaches are based on polymerization of functional monomers including unsaturated peroxides in the presence of functional chain transfer agents. That provides controlling oligomer-precursor chain length and entering reactive side and terminal groups.

The oligomer-precursors were used for construction of PA via:

– polymerization providing formation of comb-like or block-copolymers using oligomer-precursors with side or terminal peroxide groups as macroinitiators, respectively;

– polymerization providing formation of block-copolymers using oligomer-precursors with terminal hydroxyls (PEGs, polyoxazolines, fluorine alkyl alcohols, saccharides, rhamnolipids) as RedOx macroinitiators forming free radicals in reactions with Ce^{4+} salt;

– attachment of the blocks of distinct branching degree and functionality using oligomer-precursors with epoxide, amino, hydroxyl terminal groups via non-radical addition reactions.

Novel oligomer-precursors and PA of variable architectures, controlled lengths of blocks and side branches were studied using GPC, spectroscopy, and colloidal-chemical techniques. PA form SA of different degree of self-organization, size and morphology in liquids of various polarities as well as functional brushes on surfaces of polymeric and inorganic nanoparticles and flat plate surfaces, including nanofiber, of various natures. These self-assemblies are specific containers for solubilization of water-insoluble substances and nanoreactors for nucleation and functionalization of magnetic, luminescent and scintillation NPs on the surfaces. TEM, DLS, SAXS, RAMAN and luminescent spectroscopy were used for study of SA and NPs.

The developed functional nanostructures were successfully tested as vehicles for drug and nucleic acid delivery and as physically detectable cell labels and scintillators for registration of X-ray and neutron irradiation.

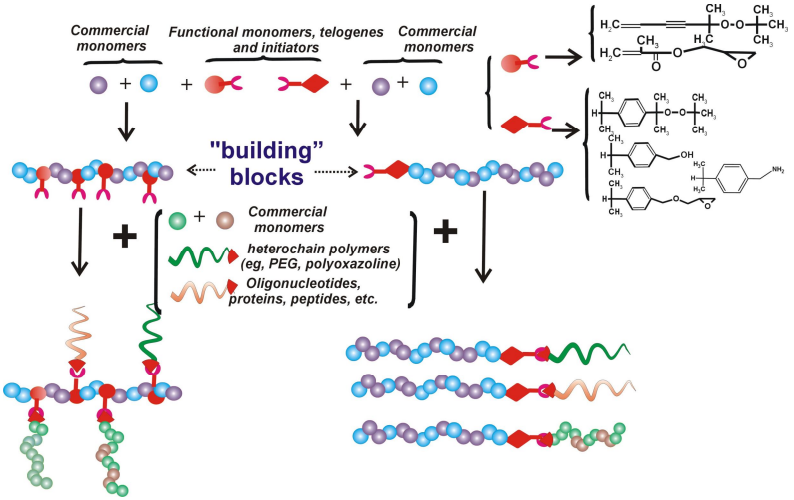

Fig. 1. General scheme of the preparing the functional polymeric amphiphils.

NON-LINEAR OPTICAL PROPERTIES OF AZULENE-, FULVENES- AND FULVALENES-BASED OLIGOMERS

Anton B. Zakharov and Vladimir V. Ivanov

Materials Chemistry Department, School of Chemistry
V. N. Karazin Kharkiv National University, 61022, Kharkiv, Ukraine
e-mail: abzakharov@karazin.ua

It is a well-know fact, that precision estimation of non-linear optical properties of π-conjugated molecules requires accurate account of electron correlation (EC) effects. For relatively small molecules (containing dozen atoms of the second period elements) post-Hartree-Fock (post-HF) *ab initio* approaches are usually employed. However, what if compound contains several hundreds of atoms? Such case is unattainable for these methods due to extremely high computational demand. Unfortunately, given problem still appears to be challenging for modern quantum chemistry.

One of the solutions is seen in the use of local theory of correlation effects. It allows to reduce the size of the task, leaving the accuracy of EC account on admissible level. Since non-linear optical response of π-conjugated systems is determined commonly by the π-shell (σ-contribution for suppressing number of compounds remains almost constant) it is rationally to consider such compounds within π-electron approximation. It allows for additional simplification of computation scheme.

According to mentioned above assumptions we implemented local π-electron variant (Pariser-Parr-Pople parameterization) of coupled cluster singles and doubles (CCSD) method with the use of the basis set of covalently unbonded ethylene (cue) [1, 2]. It allows to construct the series of approximations basing on the correlation radius value. Applicability of given approach is tested on the big number of various systems including alternant and non-alternant oligomers of different size. Carried investigation revealed however, that for some particular cases (e.g. calicene molecule, Table 1) correct description of the non-linear optical characteristics requires very high level of theory to be employed. Results are given in comparison with Full Configuration Interaction (FCI) method, in parentheses relative error (on FCI results) is given.

Table 1. Calculated components of polarizability, first and second hyperpolarizability of calicene molecule (*y* denotes longitudinal direction). Values are in *a.u.*

	α_{xx}	α_{yy}	β_{yyy}	$\gamma_{xxxx} / 10^3$	$\gamma_{yyyy} / 10^4$
HF	43.8 (9.3)	119.4 (-0.6)	-362 (-118.9)	8.05 (-15.8)	-4.74 (-20.9)
MP2	42.4 (5.7)	119.4 (-0.7)	159 (-91.7)	8.85 (-7.4)	-5.91 (-1.5)
cue-CCSD	40.2 (0.3)	123.8 (3.0)	1868 (-2.5)	9.37 (-2.0)	**-8.23 (-37.1)**
CCSD	40.3 (0.5)	121.8 (1.4)	1726 (-9.9)	9.07 (-5.1)	**-7.85 (30.8)**
CCSDT	40.2 (0.2)	120.5 (0.2)	1902 (-0.7)	9.37 (-2.0)	-6.31 (5.2)
CCSDTQ	40.1 (0.0)	120.2 (0.0)	1916 (0.0)	9.48 (-0.8)	-6.03 (0.5)
FCI	40.1	120.2	1916	9.56	-6.00

* results are taken from [1].

As can be seen, even when triples (CCSDT) are included in the calculation scheme, relative error remains on high

enough (5%) level for molecule that contains only 10 π-electrons. The error of MP2 should not be misleading, other calculations show that MP2 results are not far from HF ones.

Table 2. Calculated components of polarizability, first and second hyperpolarizability of azulene molecule (*y* denotes longitudinal direction). Values are in *a.u.*

	α_{xx}	α_{yy}	β_{yyy}	γ_{xxxx} / 10^2	γ_{yyyy} / 10^3
HF	70.17	129.21	701	4.22	-5.13
MP2	70.03	131.74	662	-2.02	-9.85
MP3	69.98	132.48	630	-3.15	-7.79
cue-CCSD	68.36	135.04	70	266	32.5
CCSD	65.38	124.80	90	189	45.7
cue-CCSDT	64.04	123.90	-179	208	42.2
CCSDT	64.01	122.94	-203	235	50.0
FCI	64.44	123.46	-173	209	44.6

Results for azulene (**Table 2**) shows that HF, MP2 and MP3 methods give values that are incorrect even by the sign and order of magnitude. Besides, for oligomers these methods show incorrect dependence of given components on the size of the system. Basing on general considerations, contribution for every periodic unit in the limit will become constant when end effects are insignificant. Despite latter consideration, methods without or with low level of EC account reveal overestimated stabilization limit. **Fig. 1** shows second hyperpolarizability dependence on the number of electrons.

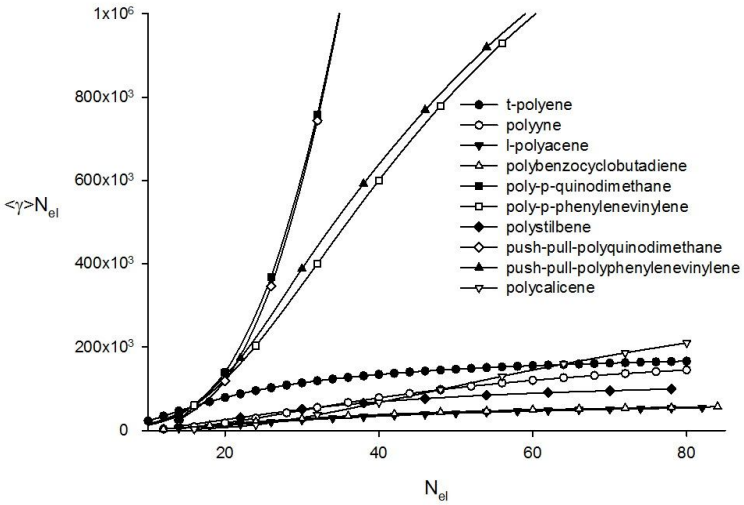

Fig. 1. Dependence of average specific second hyperpolarizability of different oligomer systems on the number of π-electrons [2].

References

1. A. Zakharov, V. Ivanov, L. Adamowicz, *J. Chem. Phys. C*, 2014, **118**, 8111.
2. A. Zakharov, V. Ivanov, L. Adamowicz, Practical Aspects of Computational Chemistry IV, 2016, 57.

TASK POTENTIAL FOR EXPERIMENTAL AND METHODOLOGICAL PREPARATION FOR FUTURE TEACHERS OF CHEMISTRY

Andrei Graboviy

Departament of Chemistry and Nanomaterials Science,
Bohdan Khmelnytsky National University,
18031, Cherkasy, Ukraine
e-mail: graboviy_ak@ukr.net

The purpose of the study is to reveal the theoretical and methodological principles of improving the experimental and methodical preparation of future chemistry teachers in the contex of a task-oriented approach to organizing the educational process in higher education.

The term "task" is used in various sciences, while practiced widely and ambiguously: how the goal is being pursued; as an order, task; as a question that needs to be solved on the basis of certain knowledge and skills; as a problem.

Analyzing the psychological content of the concept of "task", G. Ball notes that the term problem can be used to design ate objects that belong to three different categories: 1) to the categories of the object of action of the subject; 2) to the category of the situation to achieve the goal; 3) to the category of verbal for mulation of this situation [1, c.76].

Yu. Mashbits also suggests the use of the term "task" to denote three different categories of tasks: 1) tasks

(goals) of study; 2) educational tasks, or "didactic tasks" set by a teacher; 3) tasks that are provided to students in order to solve them to achieve the goals of study [5].

V. Guzeev under the task understands the diagnostic and operational purpose of the goal. The purpose is diagnostic if there are research tools for its objective verification. The purpose of the task is operational, if the wording defines the means to achieve it. Task solving involves the selection of sub tasks [4, p.13-14]. We share the point of view of the scientist, since experimental and methodical training of future teachers of chemistry can be diagnosed, the means of achievement and the separate subtasks are identified.

Thus, the purpose (task) of experimental and methodical preparation of future teachers of chemistry is the formation of experimental and methodical competencies of students regarding the organization an dimplementation of a chemical experiment in the study of chemistry in school.

The methodology of forming experimental and methodical competences is based on the activity basis, on the principle of strengthening the practical orientation of the educational process in the methodology of chemistry teaching. This principle involves involving students inactivities that are adequate to the activity of the teacher of chemistry at a comprehensive school.

Formation of experimental and methodical competencies of students inorganizing and conducting a

chemical experiment (module "Technique and methods of school chemical experiment") was carried out using the method of pedagogical design [2]. At the preparatory stage, students describe the technique and methodology of demonstration and laboratory experiments according to the plan: 1) name of the experiment; 2) reagents and equipment; 3) technique of execution: description of the experiment, drawing of the device, chemistry of processes; 4) method of use: the purpose of the experiment, the place of inclusion in the lesson, the organization of observations of students, conclusions and theoretical explanation. The technique of the experiment students are working frontal, and the methodology – the method of demonstration.

Improvement of the acquired competencies takes place while studying the module "Methodology of studying the topics of the school course of chemistry". Students prepare a synopsis of lessons using a chemical experiment, simulate the minlaboratory classes (games imulation).

Another direction of experimental and methodical preparation of future teachers of chemistry is its technology. It involves the formation of competencies of students regarding the application of teaching technologies to a chemical experiment.

In the course of scientific research, it was concluded that the educational chemical experimentis a means of implementing technologies in teaching chemistry in generaland higher educational institutions. In view of this,

we have identified a variety of learning technologies using the chemical experiment [3].

In the process of research, an activity approach to the formation of competencies was used to approach the formation of the competencies of students to apply training technology using a chemical experiment.

The research was conducted during the study of the topic "Methods of studying nitrogen, phosphorus and their compounds" (module "Methodology for studying the topics of the school course of chemistry"). Students received the task (task) to develop a chemical dictation on the topic "Ammonia, its properties". In doing so, they took advantage of the stages of pedagogical design [2].

At the preparatory stage, students analyze the task: the design object is a chemical dictation on the topic "Ammonia, its properties." At the planning stage, a list of chemical properties of ammonia was determined, which can be checked with the help of dictation. Then they analyzed in formation on the method of conducting chemical dictations. The final stage was the description of a chemical dictation.

Thus, experimental and methodical training of future teachers of chemistry is a system of diagnostically and operationally set tasks, the solution of which ensures the formation of their competencies.

References

1. G. A. Ball, About psychological content of the concept "task". *Issues of psychology*, 1970., **6**., 75–85.

2. V. S. Bezrukova, Projective pedagogy. Ekaterinburg: *Businessbook*, 1996, 344 p.
3. A. K. Graboviy, Chemical experiment and educational technologies in general educational institutions: a methodical manual for a teacher. Cherkassy: View. from ChNU named after Bohdan Khmelnytsky, 2008, 144 p.
4. V. V. Guzeev, *Chemistry in school*, 2001, **8**, 12–18.
5. E. I. Mashbits, *Soviet pedagogy*, 1973, **2**, 58–65.

PEDAGOGICAL BASES OF FORMATION OF READINESS OF FUTURE TEACHERS FOR ECOLOGICAL EDUCATION AND UPBRINGING OF STUDENTS

Tetyana Ninova

Bohdan Khmelnytsky National University of Cherkasy
e-mail: ninova@ukr.net

The modern level of ecological safety of society is connected with the level of education, culture and education of its members. Formation of ecological culture is an important social, pedagogical and universal problem. It acquires a special relevance in the modern world in implementing sustainable development education, rethinking relations in the system of "nature – man – society" and seeking ways to harmonize them. In this context, the problem of professional teacher training for future teachers of elementary school is relevant for the formation of their readiness for activities in the field of environmental education and upbringing of junior students. It should be noted that the phenomenon of readiness is the subject of study, both teachers and psychologists. The first focuses on identifying the factors and conditions, the teaching and educational tools that enable you to manage the formation and development of the future teacher. Psychologists are guided by the establishment of the nature of relationships and dependencies between the state of readiness and the effectiveness of the activity.

Purpose definition of the essence of the concept of future teachers' professional readiness for environmental education and upbringing, its structural components necessary for activities in the industry.

At different stages of work, the following methods of research were used: theoretical – analysis of psychological and pedagogical literature, content analysis of the basic concepts, generalization; observation to determine the components of the readiness of future teachers for environmental education and the upbringing of students.

In readiness for activity, we will understand the complex, integrated, systemic, personal formation (potential quality of the individual) that arises as a result of certain experience and is based on the formation of a positive attitude towards activity, awareness of motives and needs in this activity, which manifests itself in concrete actions. In the structure of the readiness of future teachers to solve the problems of environmental education and education of students on the basis of the conducted research, analysis of teachers in this field of education, we highlighted the most important components that are necessary for the future teacher of elementary school for effective activities in the field of environmental education and upbringing of the younger schoolchildren: 1) ecological culture of the teacher, according which his attitude is formed, position in the formation of the ecological culture of schoolchildren; 2) a system of philosophical, psychological and pedagogical, methodological knowledge

about the process and methods of forming the personality of schoolchildren and its important component – ecological culture; 3) system of natural sciences and environmental knowledge of students; 4) possession of the skills of organizing a holistic process of education and formation of the ecological culture of junior students.

Such a correlation of components, in our opinion, reflects the structure of the personality of the teacher-professional, and makes it possible to find out the components and indicators of his readiness for environmental education and the upbringing of students. Analysis of psychological and pedagogical literature allowed to identify the main pedagogical skills that need to be formed in future teachers of elementary school for successful activity in environmental education and education of students: gnostic, design, didactic, communicative, organizational, reflexive. Teachers training for environmental education and upbringing students is the process of mastering scientific knowledge and skills from all aspects of the interaction of nature and society and the process of forming the readiness of the teacher to solve the modern tasks of environmental education and upbringing of students, which is capable of performing in its activities such important functions: methodological, integration, cognitive-informational, motivational, predictive Level of readiness of future teachers for pedagogical activity in the field of environmental education and upbringing of students of elementary grodes determines their level of

professionalism, creative activity, responsible attitude to their work and its consequences.

The scientific novelty of the results of the study is that: based on the analysis of literary data, components are identified for the future teacher for effective activities in the field of environmental education and upbringing of junior pupils; established the main pedagogical skills and functions that should be mastered by the future teacher in the process of vocational training, which will ensure the effectiveness of their activities in the field of environmental education and upbringing.

The analysis of the psychological and pedagogical preparation of future teachers for environmental education and upbringing of students, analysis of the functions of their activity makes it possible to develop a complex of didactic conditions for the formation of the readiness of future teachers for environmental education at school, to improve the existing system of psychological and pedagogical preparation that will promote development a complex of professionally significant qualities and personality traits of a modern teacher regarding his activity in environmental education.

References

1. A. F. Lynenko, (1995) Hotovnist' maybutnikh uchyteliv do pedahohichnoyi diyal'nosti. Pedahohika i psykholohiya. (Pedagogy and psychology), 1, 125–132 (in Ukr.)

2. O. N. Pekhota, (1997) Individualization of vocational and pedagogical teacher training: dissertation of the doctor of pedagogical sciences: special 13.00.04 - Theory and Methods of Professional Education. Kyiv (in Ukr.)
3. G. V. Trotsko, (1997) Theoretical and methodological bases of students' training for educational activities in higher pedagogical educational institutions: author's abstract. dis ... doc. pedagogical sciences: special 13.00.04 Theory and Methods of Professional Education. Kyiv (in Ukr.)
4. S. U. Goncharenko, (2011) Ukrainian Pedagogical Encyclopedic Dictionary. Rivne: Volyn's Amulets (in Ukr.)
5. G. S. Tarasenko, (2006) Interrelation of aesthetic and ecological preparation of a teacher in the system of vocational education: monograph. Cherkassy: Vertical (in Ukr.)
6. A. Kolyshkina, (2016) Analiz hotovnosti vchyteliv pochakovykh klasiv do formuvannya ekolohichno dotsil'noyi povedinkyshkolyariv. Pedahohichni nauky: teoriya, istoriya, innovatsiyni tekhnolohiyi: Naukovyy Zhurnal. (Pedagogical sciences: theory, history, innovative technologies: scientific journal), 4 (58), 287–294 (in Ukr.)
7. T. M. Dovha, (2013) Transformatsiya problemy vminnya vchytys' ta yiyi vidobrazhennya v navchal'niy literaturi z pedahohiky. Naukovi zapysky

Kirovohrads'koho derzhavnoho pedahohichnoho universytetu imeni Volodymyra Vynnychenka. Pedahohichni nauky. (Scientific notes of the Volodymyr Vynnychenko Kirovograd State Pedagogical University. Pedagogical sciences). 121(1), 136–140. Rezhym dostupu: http://nbuv.gov.ua/UJRN/Nz_p_2013_121%281%29__34 (in Ukr.)

8. T. A. Sadova Professional competence and readiness for pedagogical activity: the essence and interconnection. Access mode: http://vuzlib.com/content/view/331/84/
9. S. S. Sovhir, (2009) Theoretical and Methodical Foundations of the Formation of the Ecological Worldview of Future Teachers in Higher Pedagogical Educational Institutions: author's abstract. dis ... doc. pedagogical sciences: special 13.00.04 Theory and Methods of Professional Education. Lugansk (in Ukr.)
10. Yu. Verbinenko, Professional readiness for pedagogical activity. Access mode: http://dspace.nuft.edu.ua/jspui/bitstream/123456789/12274/1/Professional.pdf (in Ukr.)

AUTHOR INDEX

Scientific Edition

BOOK OF ABSTRACTS

International Scientific Conference

MOLECULAR ENGINEERING AND COMPUTATIONAL MODELLING FOR NANO- AND BIOTECHNOLOGY: FROM NANOELECTRONICS TO BIOPOLYMERS

dedicated to the 75th anniversary of Professor Boris Minaev

September 25–26, 2018, Cherkasy, Ukraine

Signed for printing 10.09.2018. Format 60x84/16.
Headset Times
Paper offset. Cond. printed sheets 9,25. Circulation 100

Computer set and layout: Karaush-Karmazin N. M.
Publisher: Chabanenko Yu. A.
Certificate of inclusion in the state register of publishers
Series DK № 1898 of August 11, 2004
Ukraine, Cherkasy, st. O. Dashkovych 39.
Phone +38(0472) 56-46-66

Print: FOP Nechytailo O. F.
Ukraine, 18002 Cherkasy, st. O. Dashkovych 39.
Phone/fax: (0472) 37-62-60
e–mail: print@306.com.ua

Наукове видання

ЗБІРНИК ТЕЗ

Міжнародна наукова конференція

МОЛЕКУЛЯРНА ІНЖЕНЕРІЯ ТА КОМП'ЮТЕРНЕ МОДЕЛЮВАННЯ ДЛЯ НАНО- І БІОТЕХНОЛОГІЙ: ВІД НАНОЕЛЕКТРОНІКИ ДО БІОПОЛІМЕРІВ

присвяченої 75-річному ювілею професора Мінаєва Бориса Пилиповича

25–26 вересня, 2018, Черкаси, Україна

Підписано до друку 10.09.2018. Формат 60х84/16.
Гарнітура Таймс
Папір офсет. Ум. друк. арк. 9,25. Тираж 100 пр.

Комп'ютерний набір і верстка: Карауш-Кармазін Н. М.
Видавець: Чабаненко Ю. А.
Свідоцтво про внесення до державного реєстру видавців
серія ДК № 1898 від 11.08.2004 р.
Україна, м. Черкаси, вул. О. Дашкевича, 39.
Тел. (0472) 56-46-66

Друк: ФОП Нечитайло О. Ф.
Україна, 18002 м. Черкаси, вул. О. Дашкевича, 39.
Тел/факс: (0472) 37-62-60
e–mail: print@306.com.ua